



Impact of CO₂/HCO₃⁻ Availability on Anaplerotic Flux in Pyruvate Dehydrogenase Complex-Deficient *Corynebacterium glutamicum* Strains

Aileen Krüger,^a Johanna Wiechert,^a Cornelia Gätgens,^a Tino Polen,^a Regina Mahr,^b  Julia Frunzke^a

^aInstitut für Bio- und Geowissenschaften, IBG-1: Biotechnology, Forschungszentrum Jülich, Jülich, Germany

^bSenseUp GmbH, Forschungszentrum Jülich, Jülich, Germany

ABSTRACT The pyruvate dehydrogenase complex (PDHC) catalyzes the oxidative decarboxylation of pyruvate, yielding acetyl coenzyme A (acetyl-CoA) and CO₂. The PDHC-deficient *Corynebacterium glutamicum* $\Delta aceE$ strain therefore lacks an important decarboxylation step in its central metabolism. Additional inactivation of *pyc*, encoding pyruvate carboxylase, resulted in a >15-h lag phase in the presence of glucose, while no growth defect was observed on gluconeogenic substrates, such as acetate. Growth was successfully restored by deletion of *ptsG*, encoding the glucose-specific permease of the phosphotransferase system (PTS), thereby linking the observed phenotype to the increased sensitivity of the $\Delta aceE \Delta pyc$ strain to glucose catabolism. In this work, the $\Delta aceE \Delta pyc$ strain was used to systematically study the impact of perturbations of the intracellular CO₂/HCO₃⁻ pool on growth and anaplerotic flux. Remarkably, all measures leading to enhanced CO₂/HCO₃⁻ levels, such as external addition of HCO₃⁻, increasing the pH, or rerouting metabolic flux via the pentose phosphate pathway, at least partially eliminated the lag phase of the $\Delta aceE \Delta pyc$ strain on glucose medium. In accordance with these results, inactivation of the urease enzyme, lowering the intracellular CO₂/HCO₃⁻ pool, led to an even longer lag phase, accompanied by the excretion of L-valine and L-alanine. Transcriptome analysis, as well as an adaptive laboratory evolution experiment with the $\Delta aceE \Delta pyc$ strain, revealed the reduction of glucose uptake as a key adaptive measure to enhance growth on glucose-acetate mixtures. Taken together, our results highlight the significant impact of the intracellular CO₂/HCO₃⁻ pool on metabolic flux distribution, which becomes especially evident in engineered strains exhibiting low endogenous CO₂ production rates, as exemplified by PDHC-deficient strains.

IMPORTANCE CO₂ is a ubiquitous product of cellular metabolism and an essential substrate for carboxylation reactions. The pyruvate dehydrogenase complex (PDHC) catalyzes a central metabolic reaction contributing to the intracellular CO₂/HCO₃⁻ pool in many organisms. In this study, we used a PDHC-deficient strain of *Corynebacterium glutamicum*, which additionally lacked pyruvate carboxylase ($\Delta aceE \Delta pyc$). This strain featured a >15-h lag phase during growth on glucose-acetate mixtures. We used this strain to systematically assess the impact of alterations in the intracellular CO₂/HCO₃⁻ pool on growth in glucose-acetate medium. Remarkably, all measures enhancing CO₂/HCO₃⁻ levels successfully restored growth. These results emphasize the strong impact of the intracellular CO₂/HCO₃⁻ pool on metabolic flux, especially in strains exhibiting low endogenous CO₂ production rates.

KEYWORDS *Corynebacterium glutamicum*, L-valine, anaplerosis, carbon dioxide, pyruvate carboxylase, pyruvate dehydrogenase complex

Citation Krüger A, Wiechert J, Gätgens C, Polen T, Mahr R, Frunzke J. 2019. Impact of CO₂/HCO₃⁻ availability on anaplerotic flux in pyruvate dehydrogenase complex-deficient *Corynebacterium glutamicum* strains. J Bacteriol 201:e00387-19. <https://doi.org/10.1128/JB.00387-19>.

Editor Anke Becker, Philipps-Universität Marburg

Copyright © 2019 American Society for Microbiology. All Rights Reserved.

Address correspondence to Regina Mahr, r.mahr@senseup.de, or Julia Frunzke, j.frunzke@fz-juelich.de.

A.K. and J.W. contributed equally to this work.

Received 6 June 2019

Accepted 19 July 2019

Accepted manuscript posted online 29 July 2019

Published 20 September 2019

CO_2 is an inevitable product and, at the same time, an essential substrate of microbial metabolism. In water, CO_2 is in equilibrium with bicarbonate (HCO_3^-) and CO_3^{2-} , and this equilibrium is influenced by the pH of the medium (1). As products of decarboxylating reactions and substrates for carboxylation, CO_2 and HCO_3^- are involved in various metabolic processes. Consequently, the intracellular $\text{CO}_2/\text{HCO}_3^-$ pool has a significant impact on metabolic fluxes, such as anaplerosis, especially in the early phase of cultivation, when the cell density is low (2).

During aerobic growth, the pyruvate dehydrogenase complex (PDHC), which is conserved in various microbial species, catalyzes an important reaction contributing to the intracellular $\text{CO}_2/\text{HCO}_3^-$ pool (3, 4). The PDHC is a multienzyme complex belonging to the family of 2-oxo acid dehydrogenase complexes, which also include the α -ketoglutarate dehydrogenase complex and the branched-chain 2-keto acid dehydrogenase (3, 5). In particular, the PDHC catalyzes the oxidative decarboxylation of pyruvate to acetyl coenzyme A (acetyl-CoA) and CO_2 .

The Gram-positive actinobacterium *Corynebacterium glutamicum* represents an important platform strain used in industrial biotechnology for the production of amino acids, proteins, and various other value-added products (6–10). In this organism, the PDHC represents a central target for engineering the metabolic pathways of pyruvate-derived products, including L-valine, isobutanol, ketoisovalerate, and L-lysine. To this end, various studies have focused on the reduction or complete abolishment of PDHC activity in order to improve precursor availability (4, 11–13). Due to the deficiency of PDHC activity, however, cells are not able to grow on glucose as a single carbon source, a difficulty that can be circumvented by the addition of acetyl-CoA refueling substrates, such as acetate. In the presence of both carbon sources—glucose and acetate—PDHC-deficient strains initially form biomass from acetate and subsequently convert glucose into products (e.g., L-valine or L-alanine) in the stationary phase (12). In contrast to *Escherichia coli* or *Bacillus subtilis*, *C. glutamicum* does not normally show the typical diauxic growth behavior but prefers cometabolization of many carbon sources (10, 14). Coultization of glucose and acetate has been studied in detail, showing that while the consumption rates of both carbon sources decrease, total carbon consumption is comparable to that with growth on either carbon source alone, which is regulated by SugR activity (15). Further examples of sugars or organic acids with which glucose is cometabolized include fructose (16), lactate (17), pyruvate (14), and gluconate (18). It has been shown that upon growth on a mixture of glucose and acetate, the glyoxylate shunt is active and is required to fuel the oxaloacetate pool in wild-type (WT) *C. glutamicum* (15). Here it should be noted that the glyoxylate shunt is active in the presence of acetate but is repressed by glucose (19).

For growth on glycolytic carbon sources, organisms depend on tricarboxylic acid (TCA) cycle-replenishing reactions constituting the anaplerotic node (or phosphoenolpyruvate [PEP]-pyruvate-oxaloacetate node), comprising different carboxylating and decarboxylating reactions (20). Consequently, flux via these reactions is influenced by the intracellular $\text{CO}_2/\text{HCO}_3^-$ pool. In contrast to most other organisms, *C. glutamicum* possesses both anaplerotic carboxylases, namely, the PEP carboxylase (PEPCx) (EC 4.1.1.31) encoded by the *ppc* gene (21, 22) and the pyruvate carboxylase (PCx) (EC 6.4.1.1) encoded by *pyc* (20, 23). These two C_3 -carboxylating enzymes catalyze bicarbonate-dependent reactions yielding oxaloacetate from PEP or pyruvate, respectively. It has been shown that in *C. glutamicum*, these two enzymes can replace each other to a certain extent, depending on the intracellular concentrations of the respective effectors for each enzyme. However, under standard conditions during growth on glucose, the biotin-containing PCx contributes 90% of the main anaplerotic activity, in contrast to PEPCx (23). Remarkably, the Michaelis-Menten constants of both carboxylases are about 30-fold higher than those in *Escherichia coli* PEPCx (24). Apparently, a low $\text{CO}_2/\text{HCO}_3^-$ pool may thus limit anaplerotic flux, which is of special relevance in early phases, when the biomass concentration is low but high aeration may strip dissolved CO_2 from the medium.

Several studies have revealed the inhibitory effect of low partial CO_2 pressure ($p\text{CO}_2$)

on microbial growth (2, 25, 26). In the case of *C. glutamicum*, low pCO₂ led to a significant drop in the growth rate in turbidostatic continuous cultures (27) as well as in batch cultures (28). It was further demonstrated that the reduced flux through anaplerotic reactions under low CO₂/HCO₃[−] levels led to increased production of the pyruvate-derived amino acids L-alanine and L-valine (28).

While several previous studies have focused on the impact of CO₂ by altering the partial CO₂ pressure in the process, we applied targeted genetic perturbations to systematically assess the impact of the intracellular CO₂/HCO₃[−] pool on the anaplerotic flux and growth of *C. glutamicum*. In this study, we focused on PDHC-deficient strains exhibiting a reduced intracellular CO₂/HCO₃[−] pool during growth on glucose-acetate mixtures. The effect of low CO₂/HCO₃[−] levels became even more evident upon the additional deletion of the *pyc* gene, encoding the dominant anaplerotic enzyme, leading to a drastically elongated lag phase for a *C. glutamicum* $\Delta aceE \Delta pyc$ strain during growth on glucose-acetate mixtures. This effect could be attributed to reduced tolerance of glucose by these strains and was successfully complemented by the deletion of *ptsG*, encoding the glucose-specific permease of the phosphotransferase system (PTS). Remarkably, growth was successfully restored by increasing the intracellular CO₂/HCO₃[−] pool by the addition of bicarbonate, by increasing the pH, by rerouting metabolic flux over the pentose phosphate pathway (PPP), or by refueling the oxaloacetate pool by the addition of TCA cycle intermediates to the growth medium. Finally, adaptive laboratory evolution (ALE) of the *C. glutamicum* $\Delta aceE \Delta pyc$ strain on minimal medium containing glucose and acetate revealed the abolishment of glucose uptake as a key adaptive strategy to allow for growth on acetate.

RESULTS

A lowered intracellular CO₂/HCO₃[−] pool impacts the growth of PDHC-deficient strains. The pyruvate dehydrogenase complex (PDHC) contributes to a key metabolic reaction in the central metabolism by catalyzing the oxidative decarboxylation of pyruvate to acetyl-CoA (Fig. 1), thereby producing 1 molecule of CO₂ and 1 molecule of NADH per molecule of pyruvate. Previous studies have already revealed that PDHC-deficient strains feature ~2-fold-decreased excretion of CO₂ during exponential growth (29). It is therefore reasonable to assume that a reduction in the intracellular CO₂/HCO₃[−] pool has an impact on metabolic flux distribution in PDHC-deficient strains. A simple growth comparison of wild-type *C. glutamicum* and a strain lacking the *aceE* gene (and thus PDHC deficient) revealed a slightly increased lag phase for the $\Delta aceE$ strain, which became especially evident when cells were grown in microtiter plates, while the maximal growth rate appeared to be unaffected ($0.40 \pm 0.01 \text{ h}^{-1}$ for the $\Delta aceE$ strain and $0.41 \pm 0.01 \text{ h}^{-1}$ for the WT) (Fig. 2A). Remarkably, this lag phase was completely eliminated by the addition of 100 mM HCO₃[−], suggesting that the effect is attributable to the lowered intracellular CO₂/HCO₃[−] pool of this mutant (Fig. 2B).

In *C. glutamicum*, the pyruvate carboxylase (PCx) encoded by *pyc* is the dominating HCO₃[−]-dependent anaplerotic enzyme required for refueling the TCA cycle via oxaloacetate during growth on glycolytic carbon sources (23). In the next experiment, we deleted *pyc* in the $\Delta aceE$ background in order to examine the influence of different CO₂/HCO₃[−] levels on bicarbonate-dependent anaplerosis. Remarkably, the additional deletion of the *pyc* gene resulted in an elongated lag phase of about 20 h and a reduced growth rate for the $\Delta aceE \Delta pyc$ strain (maximum growth rate [μ_{\max}], $0.27 \pm 0.02 \text{ h}^{-1}$, in contrast to $0.40 \pm 0.01 \text{ h}^{-1}$ for the $\Delta aceE$ strain) during cultivation in CGXII minimal medium containing glucose and acetate (Fig. 2A). An extended lag phase was also observed for the Δpyc single mutant, but the lag phase was significantly less prominent than that for the PDHC-deficient $\Delta aceE \Delta pyc$ variant (Fig. 2C). The growth defects of both strains were successfully complemented by reintroducing the *pyc* gene on plasmid pJC1 under the control of its own promoter (Fig. 2C). Remarkably, this extended lag phase was observed only in the presence of glucose, not during cultivation on minimal medium containing acetate as the sole carbon source (Fig. 2A).

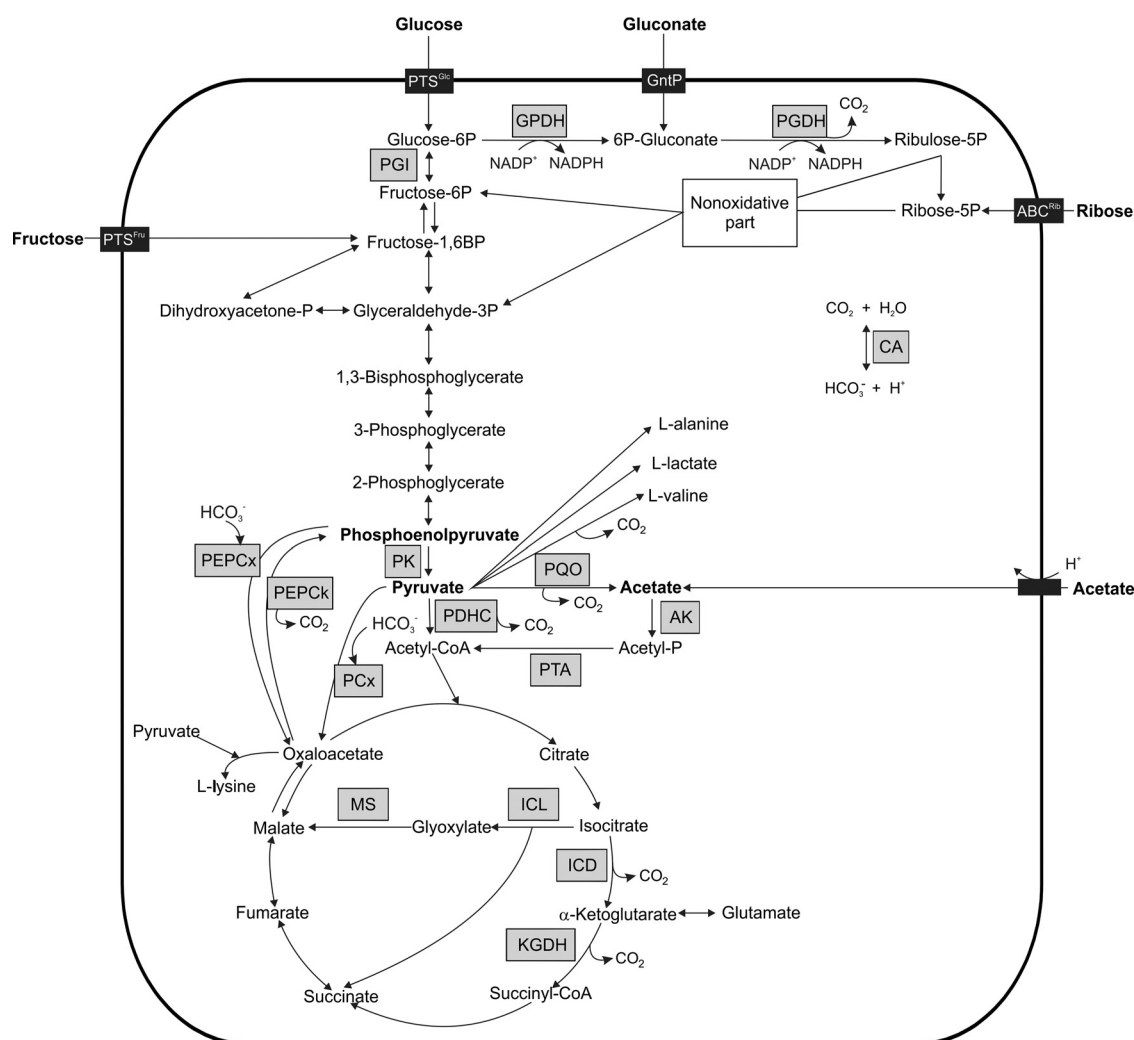


FIG 1 Schematic overview of the central carbon metabolism of *C. glutamicum*. The main aspects of glycolysis, gluconeogenesis, the pentose phosphate pathway, the TCA cycle, and anaplerosis are shown. Shaded boxes represent relevant enzymes. Carboxylation as well as decarboxylation steps are given. ABC^{Rib}, ATP-binding cassette transporter for ribose; AK, acetate kinase; CA, carbonic anhydrase; GntP, gluconate permease; GPDH, glucose-6P dehydrogenase; ICD, isocitrate dehydrogenase; ICL, isocitrate lyase; KGDH, α -ketoglutarate dehydrogenase complex; MS, malate synthase; PCx, pyruvate carboxylase; PDHC, pyruvate dehydrogenase complex; PEPCK, PEP carboxykinase; PEPcX, PEP carboxylase; PGDH, 6-phosphogluconate dehydrogenase; PGI, phosphoglucose isomerase; PK, pyruvate kinase; PQO, pyruvate:quinone oxidoreductase; PTA, phosphotransacetylase; PTS^{Glc}, permease of phosphotransferase system for glucose; PTS^{Fru}, permease of phosphotransferase system for fructose.

Glucose uptake results in strongly retarded growth in strains lacking pyruvate carboxylase. In order to determine whether glucose uptake caused the retarded growth, the $\Delta aceE \Delta pyc$ strain was cultivated in the presence of 154 mM acetate and increasing amounts of glucose (100 to 250 mM). In line with our hypothesis, the lag phase showed a stepwise increase as larger amounts of glucose were added to the medium (Fig. 3A). Accordingly, the $\Delta aceE \Delta pyc$ strain also showed significantly elongated lag phases on the PTS sugars fructose and sucrose (see Fig. S1 in the supplemental material). In contrast, the glucose concentration did not significantly affect the growth of the $\Delta aceE$ strain (Fig. 3A), in which the major anaplerotic enzyme PCx still replenishes the oxaloacetate pool.

To link the observed growth phenotype to the uptake of glucose, we deleted the *ptsG* gene, encoding the glucose-specific permease of the PTS, in the $\Delta aceE$ and $\Delta aceE \Delta pyc$ strain backgrounds. The growth and glucose consumption rates of the resulting strains were analyzed during growth on glucose and acetate. Remarkably, deletion of *ptsG* fully restored the growth of the $\Delta aceE \Delta pyc$ strain (growth rates were 0.27 ± 0.02

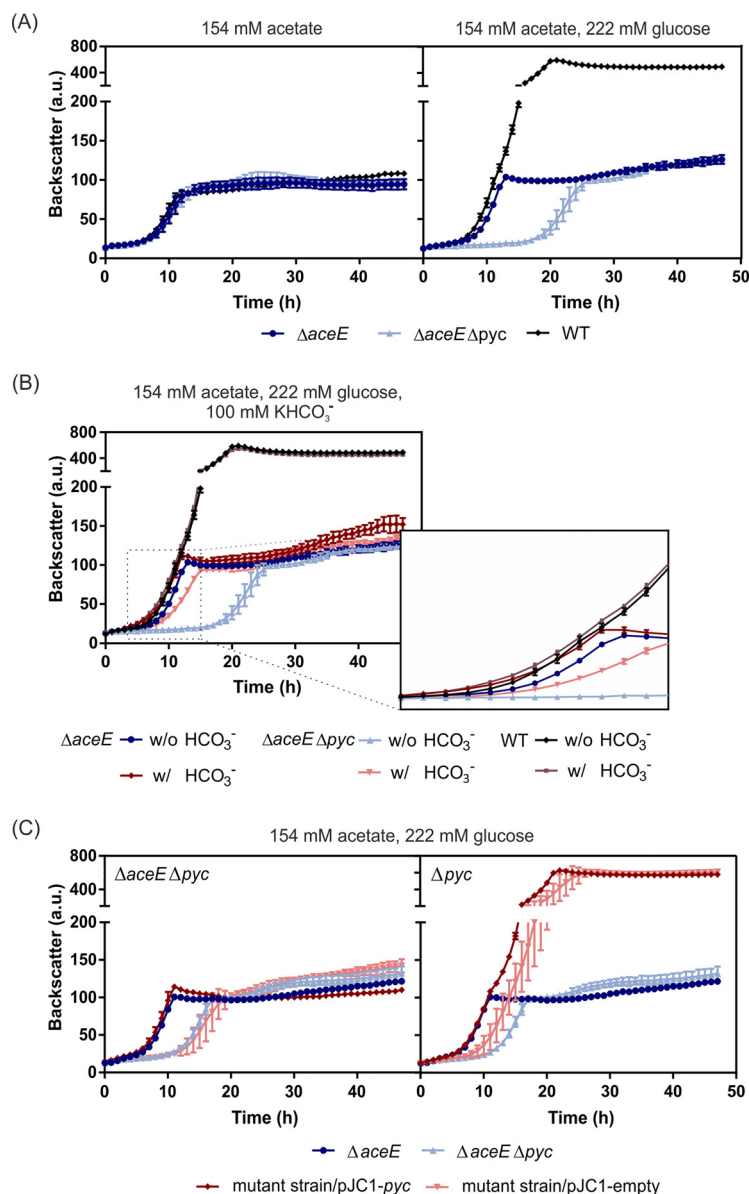


FIG 2 Impact of glucose on *aceE* and *pyc* mutant strains. The growth curves shown are based on the backscatter measurements (expressed in arbitrary units [a.u.]) in a microtiter cultivation system inoculated at an OD_{600} of 1. Data represent the averages for three biological replicates; error bars, standard deviations. (A) The *C. glutamicum* $\Delta aceE$ and $\Delta aceE \Delta pyc$ strains, as well as the wild type, were inoculated in CGXII medium containing 154 mM acetate (left) or 154 mM acetate plus 222 mM glucose (right). (B) The $\Delta aceE$ and $\Delta aceE \Delta pyc$ strains, as well as WT cells, were cultivated in CGXII medium containing 154 mM acetate and 222 mM glucose, either with (w/) or without (w/o) 100 mM KHCO_3^- . The box zooms in on the time interval between 4 h and 15 h. (C) The $\Delta aceE \Delta pyc$ (left) and Δpyc (right) strains were transformed with the pJC1-*pyc* plasmid for complementation of the *pyc* deletion or with the pJC1-empty vector as a control. Cultures were inoculated in CGXII medium containing 154 mM acetate, 222 mM glucose, and 25 $\mu\text{g}/\text{ml}$ kanamycin.

h^{-1} for the $\Delta aceE \Delta pyc$ parental strain and $0.39 \pm 0.02 \text{ h}^{-1}$ for the $\Delta aceE \Delta pyc \Delta ptsG$ strain) but resulted in reduced final backscatter values, comparable to those with growth on acetate alone (Fig. 3B). Strains lacking the *ptsG* gene consumed only minor amounts of glucose, while the $\Delta aceE$ and $\Delta aceE \Delta pyc$ strains consumed glucose after entering the stationary phase (see Fig. S2 in the supplemental material). The glucose uptake rate of the $\Delta aceE \Delta pyc$ strain, $10.87 \pm 4.95 \text{ nmol min}^{-1} \text{ g}^{-1}$, was significantly lower than that of the $\Delta aceE$ strain, $16.81 \pm 3.01 \text{ nmol min}^{-1} \text{ g}^{-1}$ (Table 1). In contrast, deletion of *ptsG* did not restore growth on either the PTS substrate fructose (see Fig.

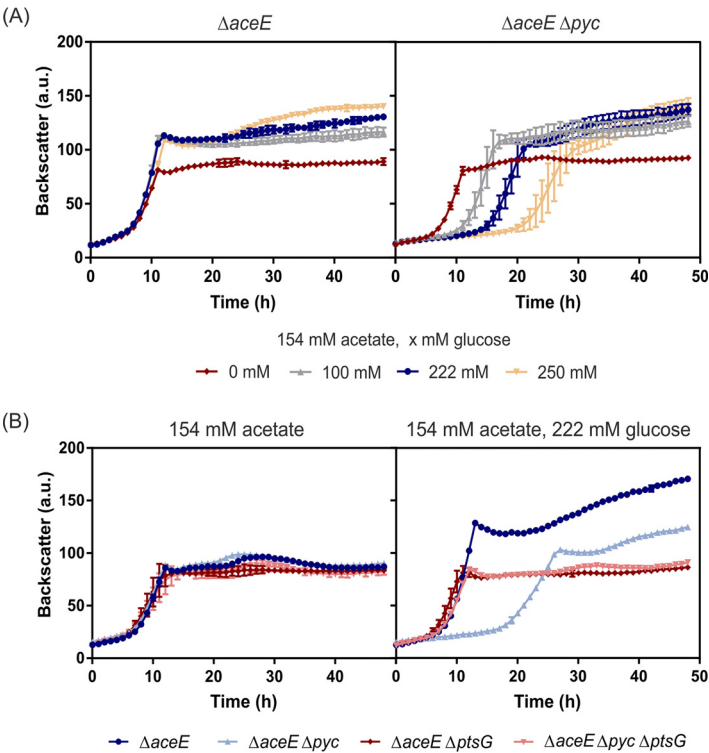


FIG 3 Influence of glucose consumption on the growth of *C. glutamicum* $\Delta aceE$ and *C. glutamicum* $\Delta aceE \Delta pyc$. The growth curves shown are based on the backscatter measurements in a microtiter cultivation system, inoculated at an OD₆₀₀ of 1. (A) The $\Delta aceE$ (left) and $\Delta aceE \Delta pyc$ (right) strains were inoculated to an OD₆₀₀ of 1 in CGXII medium containing 154 mM acetate and either no glucose or 100 mM, 222 mM, or 250 mM glucose. (B) Deletion of the *ptsG* gene in the $\Delta aceE$ and $\Delta aceE \Delta pyc$ strains restored growth on glucose-acetate mixtures relative to that for the $\Delta aceE$ and $\Delta aceE \Delta pyc$ parental strains. Data represent the averages for three biological replicates; error bars, standard deviations.

S3), which is imported mainly by the permease encoded by *ptsF* (30, 31), or the non-PTS sugar ribose (see Fig. S4). Taken together, these findings clearly link the observed growth defect of the $\Delta aceE \Delta pyc$ strain on glucose-acetate mixtures to the uptake of residual amounts of glucose.

Increased HCO₃⁻ availability improves anaplerotic flux in *pyc* mutants. Next, we used different strategies to alter the intracellular CO₂/HCO₃⁻ pool. This was achieved by (i) supplementing the medium with HCO₃⁻, (ii) mutating the endogenous urease gene producing CO₂ from urea in the early growth phase, (iii) increasing the pH of the growth medium, or (iv) rerouting metabolic flux via the pentose phosphate pathway (Fig. 4).

As with the $\Delta aceE$ parental strain, the addition of 100 mM HCO₃⁻ eliminated the lag phase for PDHC-deficient strains lacking the *pyc* gene (Fig. 2B) during microtiter plate cultivation on glucose-acetate mixtures. Restoration of growth was not possible in a

TABLE 1 Glucose consumption rates of PDHC-deficient *C. glutamicum* strains in the exponential-growth phase^a

Mutation(s)	Glucose consumption rate (nmol min ⁻¹ g ⁻¹) ^b
$\Delta aceE$	16.81 ± 3.01
$\Delta aceE \Delta pyc$	10.87 ± 4.95
$\Delta aceE \Delta ptsG$	7.24 ± 3.97
$\Delta aceE \Delta pyc \Delta ptsG$	7.32 ± 1.88

^aFor an overview of glucose consumption over the entire time course of the experiment, including the stationary phase, see Fig. S2 in the supplemental material.
^bValues are means ± standard deviations for three independent biological replicates.

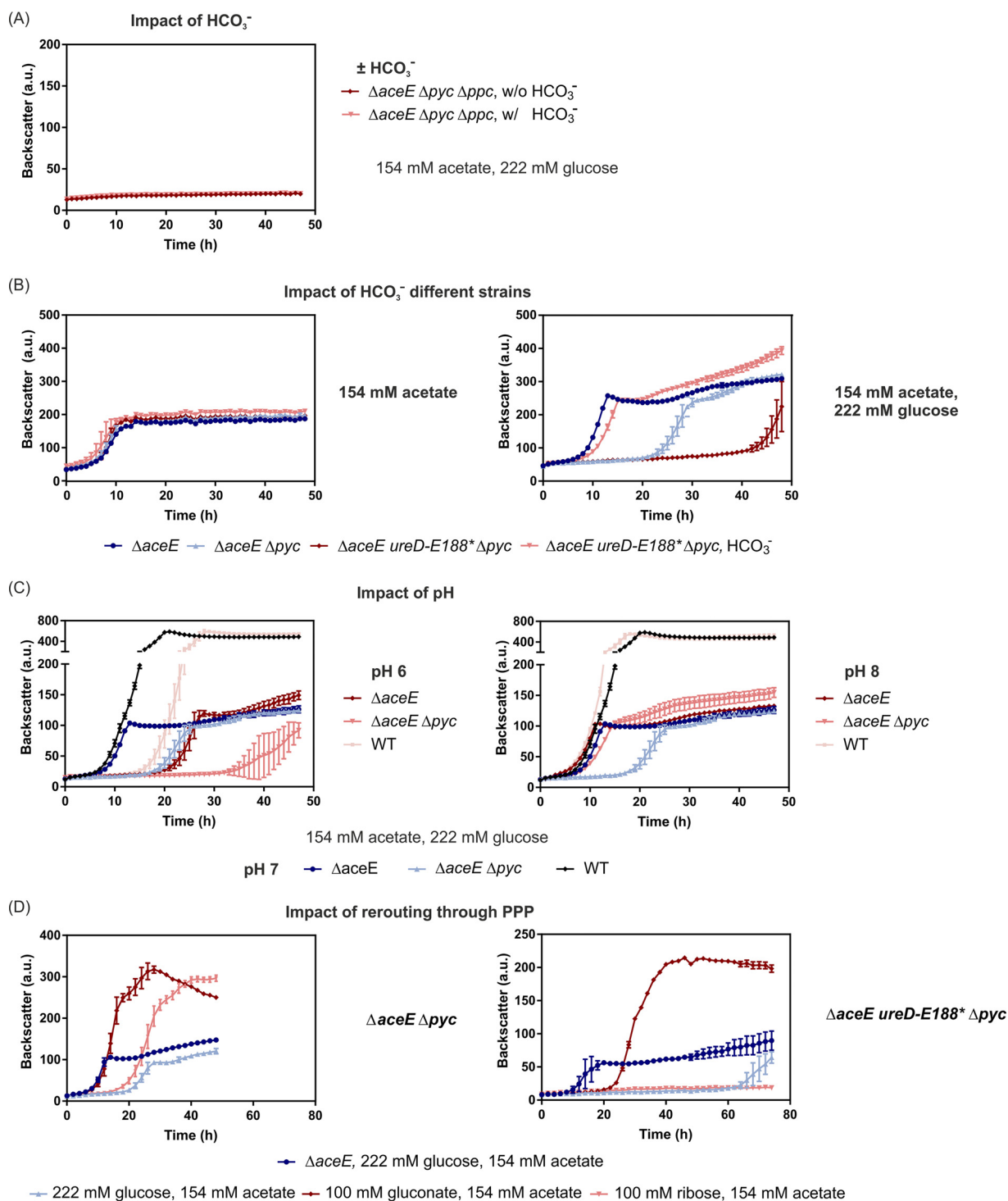


FIG 4 Increased availability of HCO_3^- improved anaplerotic flux via PEPCx in *pyc*-deficient *C. glutamicum* strains. The growth curves shown are based on the backscatter measurements in a microtiter cultivation system, inoculated at an OD_{600} of 1. Symbols represent the backscatter means for biological triplicates ($n = 3$). (A) The $\Delta aceE \Delta pyc \Delta ppc$ strain was inoculated in CGXII medium containing 154 mM acetate and 222 mM glucose (w/o HCO_3^-), and if indicated, 100 mM KHCO_3^- was added (w/ HCO_3^-). (B) The $\Delta aceE$, $\Delta aceE \Delta pyc$, and $\Delta aceE ureD-E188^* \Delta pyc$ strains were cultivated in CGXII medium containing 154 mM acetate (left) or 154 mM acetate and 222 mM glucose (right) with or without the addition of KHCO_3^- . (C) The $\Delta aceE$ and $\Delta aceE \Delta pyc$ strains, as well as the WT, were cultivated in CGXII medium containing 154 mM acetate and 222 mM glucose adjusted to a pH of 6 (left) or 8 (right), and growth was compared to that with cultivation at pH 7. (D) The $\Delta aceE$ strain and the $\Delta aceE \Delta pyc$ (left) or $\Delta aceE ureD-E188^* \Delta pyc$ (right) strain were inoculated in different growth media containing 154 mM acetate and either 222 mM glucose, 100 mM gluconate, or 100 mM ribose.

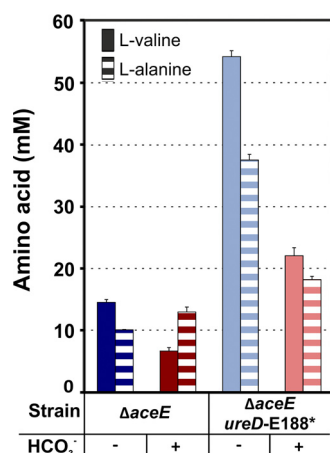


FIG 5 The intracellular CO₂-HCO₃⁻ pool significantly affects L-valine production. The influence of carbonate on the L-alanine and L-valine production of *C. glutamicum* ΔaceE and *C. glutamicum* ΔaceE ureD-E188* was investigated. Shown are L-valine and L-alanine titers in the supernatant after 28 h of cultivation in the microtiter cultivation system. Data represent average values from three independent biological replicates using uHPLC.

strain lacking both anaplerotic enzymes PCx and PEPCx, indicating that the positive effect of HCO₃⁻ on the ΔaceE Δpyc strain depends on the increased flux over PEPCx (Fig. 4A; see also Fig. S5 in the supplemental material). In contrast to the finding for PCx-deficient strains, no negative impact of glucose on the growth of the ΔaceE Δpyc strain was observed (see Fig. S6), confirming again the superior role of PCx in *C. glutamicum* (23, 32). Interestingly, we also observed a significant impact of the culture volume on the growth of the ΔaceE Δpyc strain. Since efficient liquid-air mixing continuously removes CO₂ from the culture medium, the lag phase of the ΔaceE Δpyc strain was much more prominent during microtiter plate cultivation (~17 h) than in cultures in shake flasks (a ~7-h lag phase in 100-ml cultures and a ~13-h lag phase in 50 ml) (see Fig. S7).

The urease enzyme, catalyzing the degradation of urea to ammonium and carbon dioxide, represents a further important contributor to the intracellular CO₂/HCO₃⁻ pool, especially in the early exponential phase, when cell densities and decarboxylation reaction rates are low. In a previous study, the ureD-E188* mutation was found to abolish urease activity in *C. glutamicum* and to enhance L-valine production by PDHC-deficient strains (33). In this study, we introduced the ureD-E188* mutation into the ΔaceE Δpyc background so as to examine the influence of an even lower CO₂/HCO₃⁻ level on anaplerosis in this strain background. The additional inactivation of the urease enzyme resulted in a significantly elongated lag phase of about 46 h, which could also be complemented by the addition of HCO₃⁻ (Fig. 4B), demonstrating the importance of the CO₂/HCO₃⁻ pool during the initial growth phase. Furthermore, we assessed the impact of urease mutation on the production of L-valine and L-alanine by the ΔaceE and ΔaceE ureD-E188* strains and the effect of complementation via HCO₃⁻ addition. Within 28 h of cultivation, the ΔaceE strain produced 15 mM L-valine and 10 mM L-alanine as by-products, while the ΔaceE ureD-E188* strain accumulated 54 mM L-valine and 38 mM L-alanine (Fig. 5). The addition of HCO₃⁻, however, significantly reduced L-valine production, by 54% for the ΔaceE strain and 59% for the ΔaceE ureD-E188* strain. The concentration of the by-product L-alanine increased by 22% for the ΔaceE strain and decreased by 51% for the ΔaceE ureD-E188* strain (Fig. 5). The examples of L-valine and L-alanine production illustrate the important role of the intracellular CO₂/HCO₃⁻ levels on metabolic flux in PDHC-deficient strains.

Another approach to influencing the extracellular HCO₃⁻ availability was to change the pH conditions (2). According to the Bjerrum plot, CO₂ is predominant under acidic conditions, while CO₃²⁻ is the dominant form under alkaline conditions. At a pH of

about 8, HCO₃[−] is the prevalent form. Since HCO₃[−] is the substrate of the anaplerotic enzymes PCx and PEPCx, the pH in the cultivation medium was adjusted to 8 using KOH, leading to an equilibrium shift toward higher HCO₃[−] availability. As a negative control, the pH was adjusted to 6 using HCl. While the growth of both strains tested was retarded at pH 6, it was significantly enhanced at pH 8 (Fig. 4C). Thus, elevation of the culture pH improved the growth of PDHC-deficient strains, likely by increasing anaplerotic flux.

The PPP includes another decarboxylation reaction in the central carbon metabolism, the reaction catalyzed by 6-phosphogluconate dehydrogenase (6PGDH), that contributes to the intracellular CO₂/HCO₃[−] pool. Remarkably, the lag phases of the *ΔaceE Δpyc* and *ΔaceE ureD-E188* Δpyc* strains were mostly complemented during growth on acetate and gluconate—the latter entering the PPP via gluconate-6-phosphate (Fig. 4D). Growth on ribose, which enters the PPP via ribulose-5-phosphate and thereby bypasses the decarboxylation catalyzed by 6PGDH, showed a significantly elongated lag phase in *pyc*-deficient strains (Fig. 4D). In a further experiment, metabolic/glycolytic flux was rerouted through the PPP by deleting *pgi*, encoding glucose-6-phosphate isomerase. However, deletion of *pgi* resulted in a severe growth defect in the *ΔaceE* background. In this context, the growth of the *ΔaceE Δpyc* strain featured only minor, nonsignificant improvement (see Fig. S8 in the supplemental material).

Taken together, our findings highlight the important impact of the intracellular CO₂/HCO₃[−] pool on metabolic flux in the central carbon metabolism. This is especially evident in the *ΔaceE Δpyc* strain, which lacks a central decarboxylation reaction and the key carboxylase PCx in *C. glutamicum*.

Refueling the TCA cycle improves the growth of *pyc* mutants. Glucose catabolism requires sufficient anaplerotic flux to replenish TCA cycle intermediates, providing precursors for various anabolic pathways. Therefore, we tested whether the addition of TCA cycle intermediates would complement the negative impact of glucose on the growth of the *ΔaceE Δpyc* strain. Remarkably, all TCA cycle intermediates tested (succinate, malate, citrate, and the glutamate-containing dipeptide Glu-Ala) reduced the extended lag phase of the *ΔaceE Δpyc* strain during growth on glucose-acetate mixtures (Fig. 6A). The value of Δt was defined to give the percentage change of lag phase time compared to the first doubling time of the *ΔaceE* and *ΔaceE Δpyc* strains on glucose-acetate mixtures (100%). The dipeptide Glu-Ala and succinate reduced the elongated lag phase to high extents, by 90% ($\Delta t = 10\%$) and 85% ($\Delta t = 15\%$), respectively, while the effects of citrate and malate were weaker (Δt , 40% and 38%, respectively) (Table 2).

Based on previous studies, it was known that the glyoxylate shunt might be switched off during growth on glucose-acetate mixtures, due to the inhibitory effect of glucose (34). In this study, overexpression of the *aceA* and *aceB* genes, encoding the glyoxylate shunt enzymes isocitrate lyase and malate synthase, resulted in a significantly shorter lag phase for the *ΔaceE Δpyc* strain (Fig. 6B). These genes were overexpressed by use of the pJC1 vector harboring an inducible P_{tac} promoter in front of either of two synthetic operon variants (pJC1-P_{tac}-*aceA-aceB* and pJC1-P_{tac}-*aceB-aceA*). However, it must be noted that for the *ΔaceE* strain, overexpression of *aceA* and *aceB* led to lag phases slightly longer than those with the empty-vector control (Fig. 6B). Expression from the leaky P_{tac} promoter yielded the best result, while induction with isopropyl- β -D-thiogalactopyranoside (IPTG) resulted in severe growth defects (data not shown).

Unusual intermediate accumulation or depletion can provide valuable information regarding intracellular flux imbalances causing the observed growth defects. Gas chromatography–time of flight (GC-ToF) experiments were performed for analysis of the metabolic states by comparing samples of the *ΔaceE* strain during the early-exponential phase, the *ΔaceE Δpyc* strain at the same time point during the lag phase, and the *ΔaceE Δpyc* strain during the early exponential phase (Fig. S9 in the supplemental material shows the sampling scheme). Additionally, samples of both PDHC-

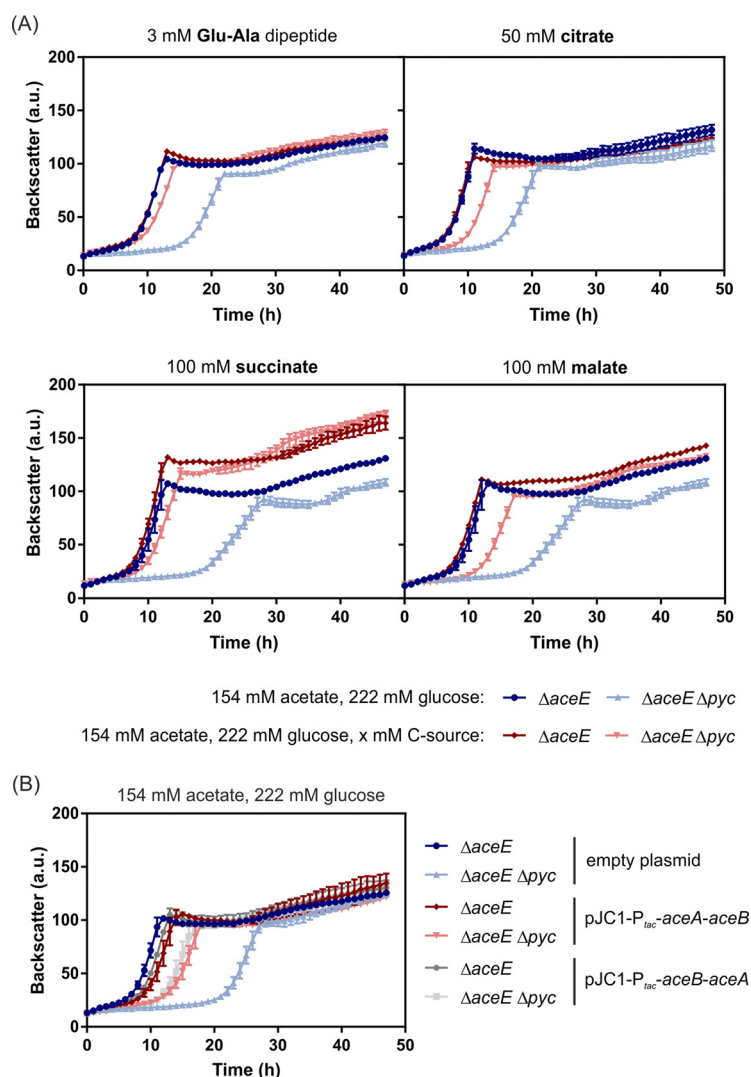


FIG 6 Refueling the TCA cycle to complement the glucose intolerance of the *ΔaceE Δpyc* strain. The growth curves shown are based on the backscatter measurements in a microtiter cultivation system, while symbols represent the backscatter means for biological triplicates ($n = 3$). The *ΔaceE* and *ΔaceE Δpyc* strains were inoculated to an OD_{600} of 1 into CGXII medium with 154 mM acetate and 222 mM glucose. (A) The TCA cycle-fueling carbon source glutamate (3 mM Glu-Ala dipeptide), citrate (50 mM), succinate (100 mM), or malate (100 mM) was added to the medium in order to analyze the effect on lag phase complementation (shades of red). As a control, growth on 154 mM acetate and 222 mM glucose is shown for the *ΔaceE* (dark blue) and *ΔaceE Δpyc* (light blue) strains in each experiment. (B) The *ΔaceE* and *ΔaceE Δpyc* strains were transformed with the pJC1-P_{tac}-*aceA-aceB* or pJC1-P_{tac}-*aceB-aceA* plasmid for simultaneous overexpression of the glyoxylate shunt enzymes isocitrate lyase (encoded by *aceA*) and malate synthase (encoded by *aceB*), while the *ΔaceE Δpyc* and *Δpyc* strains transformed with the empty pJC1 vector served as controls. Cultures were inoculated to an OD_{600} of 1 in CGXII medium containing 154 mM acetate, 222 mM glucose, and 25 μ g/ml kanamycin.

deficient strains cultivated with 100 mM HCO_3^- were measured, and WT cells in exponential phase were used as a reference (see Table S1). No significant intermediate accumulation and no occurrence of unusual compounds was observed in the lag-phase sample of the *ΔaceE Δpyc* strain relative to all other samples. Although oxaloacetate cannot be measured by this method, complete depletion of oxaloacetate-derived aspartate was detected in *ΔaceE Δpyc* cells during the lag phase but not during the exponential phase or in HCO_3^- -complemented samples. This result supports the hypothesis that oxaloacetate depletion is the key reason for the elongated lag phase.

In order to identify oxaloacetate depletion as a key growth-limiting factor and to decouple this effect from anaplerosis-dependent replenishment, the *Δpyc*, *Δpyc Δppc*,

TABLE 2 Overview of the lag phases and growth rates of the *C. glutamicum* $\Delta aceE$ and $\Delta aceE \Delta pyc$ strains cultivated with different TCA cycle carbon sources^a

Added carbon source (concn [mM])	<i>C. glutamicum</i> $\Delta aceE$			<i>C. glutamicum</i> $\Delta aceE \Delta pyc$		
	Lag phase ^b	Δt (%) ^c	Growth rate (h ^{−1})	Lag phase ^b	Δt (%) ^c	Growth rate (h ^{−1})
None	–	0	0.41 ± 0.01	+	100	0.27 ± 0.02
Glu-Ala (3)	–	0	0.35 ± 0.01	÷	10	0.33 ± 0.01
Citrate (50)	–	0	0.39 ± 0.01	÷	40	0.35 ± 0.01
Succinate (100)	–	−8	0.36 ± 0.01	÷	15	0.34 ± 0.02
Malate (100)	–	−8	0.35 ± 0.01	÷	38	0.35 ± 0.02

^aThe strains were cultivated in CGXII medium containing 154 mM acetate and 222 mM glucose with or without a TCA cycle carbon source.^b+, lag phase greater than or equal to the lag phase observed for the strain on 154 mM acetate with 222 mM glucose; ÷, shorter lag phase; –, no lag phase.^cThe difference between the first doubling time of the $\Delta aceE$ strain and that of the $\Delta aceE \Delta pyc$ strain was defined as 100%.

and $\Delta aceE \Delta pyc \Delta ppc$ strains were tested in the presence of different TCA cycle intermediates. Here, mutants lacking both anaplerotic reactions (PCx and PEPCx)—the $\Delta pyc \Delta ppc$ and $\Delta aceE \Delta pyc \Delta ppc$ strains—were not able to grow on glucose-acetate mixtures at all (Fig. 4A; also Fig. S5 in the supplemental material). Again, all TCA cycle intermediates were able to complement the glucose sensitivity of these *pyc*-deficient strains, and the growth of the $\Delta pyc \Delta ppc$ and $\Delta aceE \Delta pyc \Delta ppc$ strains was effectively restored (Table 3). Nevertheless, slight differences were observed, which might also be caused by differences in the uptake of these carbon sources.

Adaptation of *C. glutamicum* $\Delta aceE \Delta pyc$ to growth on glucose and acetate. In a previous study, Kotte et al. reported on an elongated lag phase of *E. coli* as a result of glucose-gluconeogenic substrate shifts (35). This phenomenon was ascribed to the formation of a small subpopulation that is able to start growing after carbon source switches (35). Usually, the growth of a small subpopulation is obscured by typical bulk measurements but can be visualized by single-cell approaches, such as flow cytometry (FC). To this end, the membranes of $\Delta aceE$ and $\Delta aceE \Delta pyc$ cells were stained using the nontoxic green fluorescent dye PKH67 prior to inoculation. During cellular growth, the amount of fluorescent dye is diluted by membrane synthesis, leading to a decrease in the level of single-cell PKH67 fluorescence (35). Stained $\Delta aceE$ and $\Delta aceE \Delta pyc$ cells were cultivated in minimal medium containing glucose and acetate (Fig. 7A). As a nonproliferating control, $\Delta aceE \Delta pyc$ cells were incubated in glucose as the sole carbon source. Using flow cytometry, membrane staining was analyzed during cultivation at the single-cell level (Fig. 7B). While the mean of the fluorescence of the whole $\Delta aceE$ population decreased from 2.7×10^4 arbitrary units (AU) to 7.5×10^2 AU, the mean of the fluorescence of the $\Delta aceE \Delta pyc$ population incubated in glucose medium alone shifted from 3.1×10^4 AU to 1.3×10^3 AU, resulting from a minor dilution/bleaching of fluorescence intensity during incubation. Remarkably, both the $\Delta aceE$ and $\Delta aceE \Delta pyc$ strains featured rather heterogeneous adaptation behavior on glucose-acetate mixtures, which was apparently delayed in the $\Delta aceE \Delta pyc$ strain, reflecting the elongated

TABLE 3 Overview of the lag phases and growth rates of the *C. glutamicum* Δpyc , $\Delta pyc \Delta ppc$, and $\Delta aceE \Delta pyc \Delta ppc$ strains cultivated with different TCA cycle carbon sources^a

Added carbon source (concn [mM])	Result for the <i>C. glutamicum</i> strain with the following mutation(s):					
	Δpyc		$\Delta pyc \Delta ppc$		$\Delta aceE \Delta pyc \Delta ppc$	
	Δt_{lag} (h) ^b	Growth rate (h ^{−1}) ^c	Δt_{lag} (h)	Growth rate (h ^{−1})	Δt_{lag} (h)	Growth rate (h ^{−1})
None	6 h	0.17 ± 0.02	No growth		No growth	
Glu-Ala (3)	ND	ND	8	0.21 ± 0.01	30	0.14 ± 0.01
Citrate (50)	3	0.19 ± 0.01	5	0.26 ± 0.01	8	0.20 ± 0.03
Succinate (100)	2	0.2 ± 0.02	3	0.16 ± 0.03	5	0.12 ± 0.03
Malate (100)	3	0.21 ± 0.01	17	0.18 ± 0.01	18	0.24 ± 0.01

^aStrains were cultivated in CGXII medium containing 154 mM acetate and 222 mM glucose with or without a TCA cycle carbon source.^bDifference in lag phase duration between the $\Delta aceE$ strain growing on a glucose-acetate mixture and the strain of interest growing on the respective carbon source(s). ND, not determined.^cFor comparison, the growth rate in a glucose-acetate mixture was 0.41 h^{−1} for the $\Delta aceE$ strain and 0.28 h^{−1} for the $\Delta aceE \Delta pyc$ strain in this experiment.

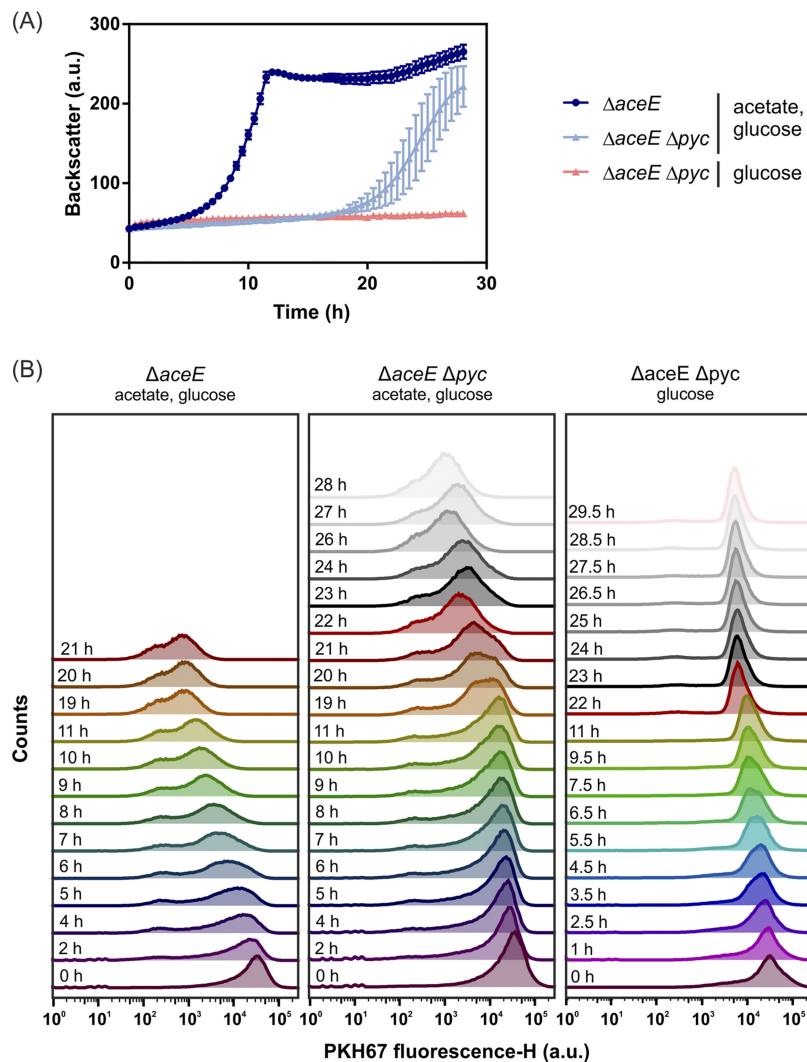


FIG 7 Heterogeneous adaptation of *C. glutamicum* $\Delta aceE$ and *C. glutamicum* $\Delta aceE \Delta pyc$ during growth on glucose and acetate. To identify a potential growing subpopulation, the fluorescent dye PKH67 was used to stain the membranes of $\Delta aceE$ and $\Delta aceE \Delta pyc$ cells prior to cultivation. The cells were cultivated in a microtiter cultivation system in the presence of 154 mM acetate and 222 mM glucose. As a nongrowing control, the $\Delta aceE \Delta pyc$ strain was additionally incubated in CGXII medium containing solely 222 mM glucose. (A) Cell growth was monitored online using a microtiter cultivation system. (B) Staining intensities were measured on the single-cell level during cultivation using flow cytometry (with three biological replicates). Shown are the frequencies of PKH67 staining intensities of one representative culture of each sample over the time course of cultivation. H, height; Counts, cell count.

lag phase. Already in the early phase of cultivation, the populations split into two subpopulations of low and high PKH67 fluorescence, indicating that only a few cells started to proliferate, while a fraction of the population was not able to grow under the same conditions (36–38).

To study the adaptation of the $\Delta aceE \Delta pyc$ strain, comparative transcriptome analyses were performed using DNA microarrays. To this end, $\Delta aceE$ and $\Delta aceE \Delta pyc$ cells were harvested at comparable optical densities (ODs) during early exponential phase (see Fig. S9 in the supplemental material). Both strains were cultivated in CGXII medium with 154 mM acetate and 222 mM glucose. Under the conditions chosen, a total of 354 genes showed significantly altered mRNA levels. While 121 genes were at least 1.7-fold upregulated ($P < 0.05$), 233 genes were 0.7-fold downregulated ($P < 0.05$) in the $\Delta aceE \Delta pyc$ strain (see Table S2). An overview of expression changes of selected genes is shown in Table 4. Among the various changes in the levels of gene expression,

TABLE 4 Comparative transcriptome analysis of *C. glutamicum* $\Delta aceE \Delta pyc$ and *C. glutamicum* $\Delta aceE$ during growth on glucose and acetate^a

Function and gene locus	Gene name	Annotation	mRNA ratio	P
PTS component				
cg1537	<i>ptsG</i>	Glucose-specific enzyme IIBC component of PTS	<u>0.59</u>	0.02
cg2117	<i>ptsI</i>	PEP:sugar phosphotransferase system enzyme I	<u>0.67</u>	0.01
cg2121	<i>ptsH</i>	Phosphocarrier protein HPr of PTS	1.16	0.11
<i>myo</i> -Inositol transport				
cg0223	<i>iolT1</i>	<i>myo</i> -Inositol transporter	1.97	0.04
cg3387	<i>iolT2</i>	<i>myo</i> -Inositol transporter	1.41	0.19
Transcriptional regulation of <i>ptsG</i>				
cg2783	<i>gntR1</i>	Transcriptional regulator, GntR family	0.76	0.05
cg1935	<i>gntR2</i>	Transcriptional regulator, GntR family	0.97	0.46
cg2115	<i>sugR</i>	DeoR-type transcriptional regulator of <i>ptsG</i> , <i>ptsS</i> , and <i>ptsF</i>	0.79	0.03
Acetate metabolism				
cg3047	<i>ackA</i>	Acetate/propionate kinase	1.99	0.01
cg3048	<i>pta</i>	Phosphate acetyltransferase	1.34	0.04
cg2560	<i>aceA</i>	Isocitrate lyase	1.70	0.12
cg2559	<i>aceB</i>	Malate synthase	1.88	0.02
Anaplerosis				
cg1787	<i>ppc</i>	Phosphoenolpyruvate carboxylase	0.91	0.32
cg3169	<i>pck</i>	Phosphoenolpyruvate carboxykinase (GTP)	0.72	0.03
cg1458	<i>odx</i>	Oxaloacetate decarboxylase	1.07	0.32
cg3335	<i>malE</i>	Malic enzyme	<u>0.48</u>	0.26
Other functions in the central carbon metabolism				
cg0973	<i>pgi</i>	Glucose-6-phosphate isomerase	<u>0.44</u>	0.03
cg2291	<i>pyk</i>	Pyruvate kinase	<u>0.59</u>	0.01
cg2891	<i>pqo</i>	Pyruvate:quinone oxidoreductase	<u>0.47</u>	0.02

^aThe expression of selected genes encoding central metabolic enzymes or regulators is given as the ratio of the mRNA level in the $\Delta aceE \Delta pyc$ strain to that in the $\Delta aceE$ strain. mRNA ratios of ≤ 0.70 are underlined, and mRNA ratios of ≥ 1.70 are shown in boldface. *P* values of > 0.05 (from three biological replicates) are italicized. For the complete data set, see Table S4 in the supplemental material.

we observed 0.59-fold and 0.67-fold downregulation of the PTS components *ptsG* and *ptsI*, respectively, in the $\Delta aceE \Delta pyc$ strain, in line with the decreased glucose uptake rates of this strain (Table 1). In contrast, *iolT1*, encoding the *myo*-inositol transporter, which is responsible, *inter alia*, for PTS-independent glucose uptake, was upregulated (39, 40). This is in line with the fact that the *ptsG*-deficient strains still consumed minor amounts of glucose. Interestingly, genes involved in acetate metabolism, including *aceA* and *aceB*, constituting the glyoxylate shunt, displayed increased mRNA levels in the $\Delta aceE \Delta pyc$ strain. This may also represent an important adaptive mechanism, since the glyoxylate shunt needs to be active in the $\Delta aceE \Delta pyc$ strain to compensate for the loss of TCA cycle intermediates during coconsumption of acetate and glucose, as demonstrated by the effect of *aceA-aceB* overexpression in this study (Fig. 6B). While the mRNA levels of genes encoding anaplerotic enzymes did not show significant changes, the glycolytic genes *pgi* and *pyk* featured ~ 2 -fold-reduced levels in the $\Delta aceE \Delta pyc$ mutant. This might well reflect an adaptive mechanism, since downregulation of *pyk* would reduce flux from PEP to pyruvate, and reduced expression of *pgi* would probably lead to increased flux through the PPP, contributing an additional decarboxylation step.

Less is more: ALE of the $\Delta aceE \Delta pyc$ strain reveals rapid inactivation of glucose uptake. In order to identify key mutations abolishing the lag phase of the $\Delta aceE \Delta pyc$ strain, an adaptive laboratory evolution (ALE) experiment was performed. In this ALE experiment, *C. glutamicum* $\Delta aceE \Delta pyc$ was grown in CGXII minimal medium containing 154 mM acetate and 222 mM glucose in 16 repetitive-batch cultures overall. Remarkably, after 8 inoculations, a significantly shortened lag phase was already observed; after 10 inoculations, the $\Delta aceE \Delta pyc$ strain featured a lag phase similar to that of the

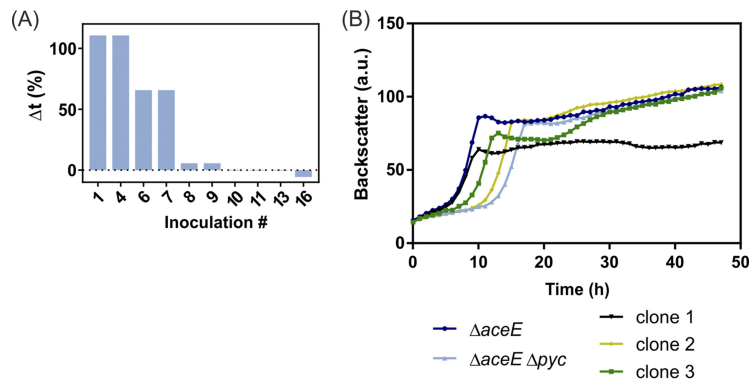


FIG 8 Adaptive laboratory evolution of *C. glutamicum* $\Delta aceE \Delta pyc$. Growth was analyzed for single inoculation steps obtained from the adaptive laboratory evolution (ALE) approach, which was performed with the $\Delta aceE \Delta pyc$ strain in the presence of glucose and acetate. Growth curves are shown based on the backscatter measurements in a microtiter cultivation system. Symbols represent the backscatter means. (A) For growth analysis on the population level, glycerol stocks prepared during the ALE experiment were used for the inoculation of a first preculture in BHI medium supplemented with 51 mM acetate. The second preculture, in CGXII medium containing 154 mM acetate, was then used for inoculation of the main culture in CGXII medium containing 154 mM acetate and 222 mM glucose (starting OD_{600} 1). Shown is the development of the relative lag phase duration after repetitive inoculations of the $\Delta aceE \Delta pyc$ strain in media containing glucose and acetate. The difference in the first doubling time between the $\Delta aceE$ and $\Delta aceE \Delta pyc$ strains was set to 100%. For each inoculation, the difference in the lag phase from that for the $\Delta aceE$ strain was calculated and is given as a percentage. (B) Single clones were isolated from batches 7 (clone 1), 8 (clone 2), and 10 (green) and were cultivated as described above. The $\Delta aceE$ and $\Delta aceE \Delta pyc$ strains served as controls. These single clones were further analyzed by genome sequencing (Table 5).

$\Delta aceE$ strain (Fig. 8A). In contrast, serial cultivation transfers in CGXII medium containing solely acetate did not lead to improved growth in a glucose-acetate medium, indicating that glucose exerted evolutionary selection pressure (see Fig. S10 in the supplemental material). Genome resequencing of the three selected glucose-acetate clones for which data are presented in Fig. 8B revealed mutations in the *ptsI* gene, encoding the EI enzyme of the PTS, in two independently evolved clones (Table 5). This is in agreement with the reduced biomass formation of both clones, in which glucose uptake was apparently abolished to optimize growth on acetate. The third clone showed only slightly accelerated growth, but biomass formation was not impaired. Here, sequencing revealed a mutation in the *rpsC* gene, encoding the ribosomal S3 protein.

In summary, it was indeed possible to eliminate the observed lag phase of the $\Delta aceE \Delta pyc$ strain ascribed to glucose sensitivity by an adaptive laboratory evolution approach. Especially, the mutations identified in the *ptsI* gene are in agreement with other experiments emphasizing the high selective pressure exerted by glucose on PCx-deficient strains when the intracellular HCO_3^- levels are limiting.

DISCUSSION

During growth on glucose, the pyruvate dehydrogenase complex catalyzes a central metabolic reaction contributing to the intracellular CO_2/HCO_3^- pool. In this study, we systematically perturbed the intracellular CO_2/HCO_3^- pool of PDHC-deficient *C. glutamicum* strains in order to monitor the impact on growth and anaplerotic flux. Even the PDHC-deficient strain *C. glutamicum* $\Delta aceE$ features a slightly elongated lag phase on glucose-acetate mixtures relative to that of the wild type, while no difference in growth is observed when strains are growing on gluconeogenic substrates, such as acetate.

TABLE 5 Key mutations identified in an adaptive laboratory evolution experiment with *C. glutamicum* $\Delta aceE \Delta pyc$

Clone no.	Batch no.	Gene locus	Gene name	Annotation	Mutation
1	7	cg2117	<i>ptsI</i>	EI enzyme, general component of PTS (EC 2.7.3.9)	Exchange, R132H
2	8	cg0601	<i>rpsC</i>	30S ribosomal protein S3	Exchange, R225H
3	10	cg2117	<i>ptsI</i>	EI enzyme, general component of PTS (EC 2.7.3.9)	Exchange, G15S

This is remarkable, since this strain catabolizes only a minor fraction of the glucose provided in the exponential-growth phase but turns to the production of L-valine and L-alanine from glucose in the stationary phase (11, 12). The growth defect of *C. glutamicum* $\Delta aceE$ was, however, successfully complemented by the addition of HCO₃[−], which had no significant effect on the growth of wild-type cells, thus hinting at problems caused by impaired anaplerotic flux in this strain background. By comparing the CO₂ production rates of the *C. glutamicum* $\Delta aceE$ strain and the wild type, Bartek et al. were able to show in a previous study that the $\Delta aceE$ strain excretes only around 0.83 mmol of CO₂ g^{−1} h^{−1}, while the wild type excretes ca. 1.65 mmol of CO₂ g^{−1} h^{−1} (29). The lower CO₂ production rates of the PDHC-deficient strain already indicate a significant impact on the intracellular CO₂/HCO₃[−] pool affecting metabolic flux distribution, especially at low cell densities, when CO₂/HCO₃[−] is limiting.

The anaplerotic node comprises the essential link between glycolysis/gluconeogenesis and the TCA cycle (20). In contrast to most other organisms, *C. glutamicum* possesses both anaplerotic carboxylases, PEPCx (encoded by *ppc*) and PCx (encoded by *pyc*), catalyzing the anaplerotic bicarbonate-dependent reactions to yield oxaloacetate from PEP or pyruvate, respectively. It was shown that in *C. glutamicum*, these two enzymes can replace each other to a certain extent, depending on the intracellular concentrations of the respective effectors for each enzyme. However, during growth on glucose, the biotin-containing PCx contributes 90% to the main anaplerotic activity, in contrast to PEPCx (23, 32). In our study, deletion of the *pyc* gene resulted in a severely elongated lag phase (>15 h) of the $\Delta aceE \Delta pyc$ strain when glucose was present in the medium. Retarded growth of Δpyc strains has been observed previously, and in line with our data, other studies also reported a severe growth defect of a Δpyc strain under low CO₂/HCO₃[−] levels (23, 28). This effect appeared to be even more severe when the cells were grown in microtiter plates under CO₂-stripping conditions (low culture volume, high air mixing) than when they were grown in higher culture volumes (see Fig. S7 in the supplemental material). The PDHC-deficient mutant strain *C. glutamicum* $\Delta aceE \Delta pyc$ was found to react very sensitively to small changes in intracellular bicarbonate availability and was therefore used as a test platform with which to assess systematically the impact of perturbations affecting the intracellular CO₂/HCO₃[−] pool. While addition of HCO₃[−], an increase in the pH, and higher culture volumes rescued the strain, mutation of the urease accessory protein (*ureD*-E188*), which lowers the intracellular CO₂/HCO₃[−] pool, resulted in an even more severe phenotype. It was not possible to restore growth if the second anaplerotic gene, *ppc*, was deleted as well, confirming that the measures mentioned above fostered the flux over the remaining anaplerotic reaction catalyzed by PEPCx.

The mutation in *ureD* was revealed by a previous biosensor-driven evolution approach selecting for mutations enhancing L-valine production in *C. glutamicum* (33). In that study, inactivation of the urease enzyme by the *ureD*-E188* mutation reduced the anaplerotic flux via PCx, resulting in increased precursor availability of pyruvate-derived products, such as L-valine and L-alanine (33). In the present study, we confirmed this finding by complementation with HCO₃[−], counteracting the effect of the *ureD*-E188* mutation. In another study, by Blombach et al., lower CO₂/HCO₃[−] levels also triggered enhanced production of L-valine and L-alanine by *C. glutamicum* during shake flask cultivation (28). However, a positive impact of anaplerotic reactions has been confirmed for other products, for example, oxaloacetate-derived products, such as L-lysine. In those studies, attempts to overexpress *pyc* or the introduction of deregulated variants significantly improved L-lysine production (41, 42). However, in spite of great efforts and success in the development of L-lysine production strains, the impact of altered CO₂/HCO₃[−] levels has not been systematically assessed so far.

Residual glucose consumption by PDHC-deficient *C. glutamicum* strains has already been reported in previous studies (11, 12, 29). The results of this work, however, emphasize that mutants lacking the major anaplerotic route via PCx (Δpyc mutants) are under strong evolutionary pressure in the presence of glucose. Although the strains would be able to grow on the acetate supplied in the growth medium, increasing levels

of glucose resulted in a severely elongated lag phase (as long as >40 h with 250 mM) for *C. glutamicum* $\Delta aceE \Delta pyc$. Besides the above-mentioned efforts to increase the CO_2/HCO_3^- pool, the deletion of the *ptsG* gene itself effectively restored growth on glucose but not on other PTS substrates and not on ribose. These results indicate that growth retardation is not the result of PtsG-dependent regulation as known for *E. coli* (43, 44).

Furthermore, among the three key mutations identified in the ALE experiment, two single nucleotide polymorphisms (SNPs) obtained from independent cell lines were located within the *ptsI* gene, encoding the EI component of the PTS. These findings clearly highlight the problems of residual glucose consumption in strains featuring impaired anaplerotic flux. One reason for the observed growth phenotype might be stress resulting from the intracellular accumulation of sugar phosphates. In *Escherichia coli*, sugar phosphate stress can be caused by the accumulation of any sugar phosphates due to a block in glycolysis (45), e.g., by mutations in *pgi* or *pfkA* (46), or due to excessive glucose uptake caused, e.g., by overexpression of *uhpT*, encoding a sugar phosphate permease (47). The resulting metabolic imbalance causes growth inhibition. For example, in *C. glutamicum*, accumulation of several sugar phosphates, such as fructose-1,6-bisphosphate or PEP, inhibits the key enzyme of the glyoxylate shunt, isocitrate lyase, already at low concentrations (34). To counteract this stress, *E. coli* triggers SgrR, which, in turn, activates SgrS by an unknown signal. The transcription factor SgrS then prevents further uptake of glucose by downregulation of *ptsG* (45, 48, 49). This is in line with the finding of our study showing a slight downregulation of *ptsG* upon resumed growth of the $\Delta aceE \Delta pyc$ strain (Table 4). This reduction of glucose uptake via the PTS, which converts PEP to pyruvate during glucose transport, also contributes to increased PEP availability for the remaining anaplerotic reaction catalyzed by PEPCx. Further, this is in line with an upregulation of *iolT1*, which ensures minor usage of glucose without PEP depletion (39, 40). In this context, the downregulation of the *pyk* gene in the $\Delta aceE \Delta pyc$ strain can also be interpreted as a potential adaptation to increase the PEP pool, fostering anaplerotic flux. All these strategies counteracting PEP depletion underline the fact that under these conditions, the anaplerotic enzyme PEPCx is not able to deliver appropriate amounts of oxaloacetate in the $\Delta aceE \Delta pyc$ strain.

During growth on gluconeogenic carbon sources—such as acetate—the transcriptional repressor SugR represses the expression of the PTS genes in *C. glutamicum*, including the glucose-specific *ptsG* gene but also *ptsF*, *ptsS*, and general components, such as *ptsI* and *ptsH* (50–52). Derepression appears to be triggered by the accumulation of fructose-6-phosphate (F6P), which is generated from glucose-6-phosphate entering glycolysis. Consequently, F6P accumulation leads to an increase in glucose consumption rates, resulting in parallel catabolization of glucose and acetate (15). The fact that the PDHC-deficient strains are also subject to regulation by SugR has been demonstrated by studies showing that the $\Delta aceE \Delta sugR$ strain leads to glucose consumption rates as much as 4-fold higher (53).

In aerobic glucose-based bioprocesses, the endogenous production of CO_2 is typically sufficiently high to promote microbial growth even at low cell densities. However, it is well known that the anaerobic growth of some bacteria, such as *E. coli*, requires an external supply of CO_2/HCO_3^- to avoid long lag phases (25, 54, 55). The critical impact of CO_2/HCO_3^- levels may become especially evident under conditions where the endogenous CO_2 production rate becomes limiting. This was nicely demonstrated by a recent study of Bracher et al., who showed that long lag phases of engineered, but nonevolved, *Saccharomyces cerevisiae* strains during xylose fermentation could be avoided by sparging the bioreactor cultures with CO_2-N_2 mixtures (56). Alternatively, the addition of L-aspartate, whose transamination provides oxaloacetate, which refuels the TCA cycle, completely abolished the long adaptation phase of the respective yeast strains. In line with these findings, a recent ^{13}C flux analysis with *E. coli* revealed that considerable turnover of lipids via β -oxidation appears to be required for growth on xylose to enhance the intracellular CO_2/HCO_3^- pool to a growth-promoting level that

enables anaplerotic flux (57). These findings are in good agreement with our demonstration in this study that the elongated lag phase of the *C. glutamicum* $\Delta aceE \Delta pyc$ strain can be eliminated by various measures, either by increasing the intracellular CO₂/HCO₃⁻ level or by refueling the TCA cycle with various intermediates, such as citrate, malate, or succinate.

Overall, oxaloacetate depletion appeared to represent a key issue causing the delayed growth of the $\Delta aceE \Delta pyc$ strain. Our data revealed that this is caused by impaired anaplerotic flux on glucose due to low intracellular CO₂/HCO₃⁻ levels as well as reduced activities of glyoxylate cycle enzymes. As known from several organisms, the activity of glyoxylate shunt enzymes is tightly repressed during growth on glucose. In *C. glutamicum*, the transcription of *aceA* (encoding isocitrate lyase) and *aceB* (encoding malate synthase) is repressed by RamB in the presence of glucose (58) and is activated by RamA in the presence of acetate (59). The PDHC-deficient strains in this study were grown on glucose-acetate mixtures. In an earlier study by Wendisch et al., it was emphasized that the anaplerotic function is entirely achieved by the glyoxylate cycle enzymes when wild-type *C. glutamicum* is grown on glucose plus acetate (15). They further revealed that this function can be partly complemented by PEPCx or PCx (15). However, the possibility remains that the glyoxylate cycle enzymes, especially isocitrate lyase, are repressed in the PDHC-deficient mutants due to accumulation of, e.g., sugar phosphates caused by the PDHC and/or *pyc* inactivation. Reinscheid et al. (1994) claimed that the sugar phosphates 3-phosphoglycerate, 6-phosphogluconate, and fructose 1,6-bisphosphate cause inhibition of the isocitrate lyase in *C. glutamicum* (34). Although transcriptional regulation of the glyoxylate shunt is different, isocitrate lyases of *E. coli* are also repressed by glucose catabolites (60–62). Consequently, a repressed glyoxylate shunt due to glucose catabolite accumulation probably also accounts for oxaloacetate depletion in PDHC-deficient strains; this is especially problematic for the $\Delta aceE \Delta pyc$ strain, which cannot complement this depletion by anaplerotic pathways due to lower intracellular CO₂/HCO₃⁻ levels.

Taken together, these results emphasize the important impact of the intracellular CO₂/HCO₃⁻ pool on metabolic flux distribution, which is especially relevant in engineered strains exhibiting lower endogenous CO₂ production rates, as exemplified by PDHC-deficient strains in this study, but also by the performance of pentose-fermenting yeast and *E. coli* strains (56, 57). Consequently, the lack of an important by-product, such as CO₂ released by the PDHC, may have a significant impact on cellular metabolism and growth, especially on glycolytic substrates demanding high flux via anaplerotic reactions.

MATERIALS AND METHODS

Bacterial strains and growth conditions. All bacterial strains and plasmids used in this study are listed in Tables 6 and 7, respectively. Mutant strains are based on the wild-type *Corynebacterium glutamicum* strain ATCC 13032 (63).

Standard cultivation of *C. glutamicum* $\Delta aceE$ cells and derivatives was performed on brain heart infusion (BHI; Difco; BD, Heidelberg, Germany) agar plates containing 51 mM potassium acetate (referred to here as acetate) (ChemSolute; Th. Geyer, Stuttgart, Germany) at 30°C for 2 days. One single colony was picked and was incubated for 8 to 10 h at 30°C in either 4.5 ml or 1 ml BHI containing 154 mM acetate in reaction tubes or deep-well plates (VWR International, PA, USA), respectively. First precultures were used to inoculate second precultures in CGXII minimal medium (64) supplemented with 154 mM acetate either as 10-ml cultures in shake flasks or in 1-ml volumes in deep-well plates. After overnight growth, a main culture was inoculated at an optical density at 600 nm (OD₆₀₀) of 1 in CGXII medium containing 154 mM acetate and either 222 mM D-(+)-glucose monohydrate (Riedel-de Haën, Seelze, Germany) (referred to here as glucose) or any other carbon source as stated, e.g., D-(+)-fructose (Sigma-Aldrich, Taufkirchen, Germany) (referred to as fructose), D-(+)-sucrose (Roth, Karlsruhe, Germany) (referred to as sucrose), D-gluconic acid sodium salt (Sigma-Aldrich, Taufkirchen, Germany) (referred to as gluconate), D-(+)-ribose (Sigma-Aldrich, Taufkirchen, Germany) (referred to as ribose), citric acid monohydrate (Merck Millipore, Darmstadt, Germany) (referred to as citrate), H-Glu-Ala-OH (Bachem AG, Bubendorf, Switzerland) (referred to as Glu-Ala), succinic acid (Sigma-Aldrich, Taufkirchen, Germany) (referred to as succinate), or L-malic acid (Merck Millipore, Darmstadt, Germany) (referred to as malate). To increase the extracellular availability of bicarbonate, 100 mM potassium HCO₃⁻ (Merck Millipore, Darmstadt, Germany) was added to the basic CGXII solution. The pH was adjusted to 7, and subsequently, the medium was passed through a sterile filter before inoculation. In order to analyze the effects of different pH levels, either HCl (to lower the pH) or KOH (to increase the pH) was added to the CGXII basis, which was sterile

TABLE 6 Bacterial strains used in this study

Strain	Characteristics	Source or reference
<i>C. glutamicum</i>		
ATCC 13032	Wild type, biotin auxotroph	S. Kinoshita et al. (77)
$\Delta aceE$ strain	ATCC 13032 derivative with deletion of <i>aceE</i>	M. E. Schreiner et al. (5)
$\Delta aceE \Delta pyc$ strain	ATCC 13032 derivative with deletions of <i>aceE</i> and <i>pyc</i>	This work
$\Delta aceE \Delta ptsG$ strain	ATCC 13032 derivative with deletions of <i>aceE</i> and <i>ptsG</i>	This work
$\Delta aceE \Delta pyc \Delta ptsG$ strain	ATCC 13032 derivative with deletions of <i>aceE</i> , <i>pyc</i> , and <i>ptsG</i>	This work
$\Delta aceE \Delta pgi$ strain	ATCC 13032 derivative with deletions of <i>aceE</i> and <i>pgi</i>	This work
$\Delta aceE \Delta pyc \Delta pgi$ strain	ATCC 13032 derivative with deletions of <i>aceE</i> , <i>pyc</i> , and <i>pgi</i>	This work
$\Delta aceE \Delta ppc$ strain	ATCC 13032 derivative with deletions of <i>aceE</i> and <i>ppc</i>	This work
$\Delta aceE \Delta pyc \Delta ppc$ strain	ATCC 13032 derivative with deletions of <i>aceE</i> , <i>pyc</i> , and <i>ppc</i>	This work
$\Delta aceE ureD$ -E188* strain	ATCC 13032 derivative with deletion of <i>aceE</i> and with <i>ureD</i> -E188* (Glu188 replaced by the stop codon)	R. Mahr et al. (33)
$\Delta aceE ureD$ -E188* Δpyc strain	ATCC 13032 derivative with deletions of <i>aceE</i> and <i>pyc</i> and with <i>ureD</i> -E188* (Glu188 replaced by the stop codon)	This work
Δpyc strain	ATCC 13032 derivative with deletion of <i>pyc</i>	P. G. Peters-Wendisch et al. (23)
$\Delta pyc \Delta ppc$ strain	ATCC 13032 derivative with deletions of <i>aceE</i> and <i>ppc</i>	A. Schwentner et al. (78)
<i>E. coli</i> DH5 α	F ⁻ $\phi 80lacZ\Delta M15 \Delta(lacZYA-argF)U169 recA1 endA1 hsdR17(r_K^- m_K^+)$ <i>phoA supE44 thi-1 gyrA96 relA1</i> λ^- ; for general cloning purposes	Invitrogen

filtered afterwards. For cultivations in the presence of TCA cycle-filling/refueling substrates, 50 mM citric acid monohydrate (citrate), 3 mM H-Glu-Ala-OH dipeptide (Glu-Ala), 100 mM succinic acid (succinate), or 100 mM L-malic acid (malate) was used. In experiments where gluconate or ribose was used as the carbon source, 100 mM D-gluconic acid sodium salt or 100 mM D-ribose was added, respectively. Biomass formation was monitored during cultivation in shake flasks by measuring the OD₆₀₀ or by measuring backscatter values during microtiter plate cultivation. Where necessary, the medium was also supplemented with 25 μ g/ml kanamycin.

Escherichia coli DH5 α was used for cloning and plasmid isolation. Cells were directly inoculated from a glycerol stock or from a lysogeny broth (LB) agar plate and were grown in shake flasks in LB medium at 37°C. If necessary for selection, the medium was also supplemented with 50 μ g/ml kanamycin.

TABLE 7 Plasmids used in this study

Plasmid	Characteristics	Source or reference
pK19mobsacB	Contains negative (<i>sacB</i>) and positive (Kan ^r) selection markers for genomic integration and deletion	A. Schäfer et al. (70)
pK19mobsacB- Δpyc	Kan ^r ; derivative of pK19mobsacB for partial <i>pyc</i> gene deletion, containing only the first 499 bp and last 493 bp of <i>pyc</i> , with the deletion of 2,429 bp in the middle	P. G. Peters-Wendisch et al. (23)
pK19mobsacB- $\Delta ptsG$	Kan ^r ; derivative of pK19mobsacB for partial <i>ptsG</i> gene deletion, containing only the last 491 bp of <i>ptsG</i> , with the deletion of the first 1,561 bp	This work
pK19mobsacB- Δpgi	Kan ^r ; derivative of pK19mobsacB for <i>pgi</i> gene deletion, containing only the last 537 bp of <i>pgi</i> , with the deletion of the first 1,086 bp	This work
pK19mobsacB- Δppc	Kan ^r ; derivative of pK19mobsacB for partial <i>ppc</i> gene deletion, containing only the first 391 bp and last 447 bp of <i>ppc</i> , with the deletion of 1,922 bp in the middle	J. Buchholz et al. (13)
pK19mobsacB- <i>ureD</i> -E188*	Kan ^r ; derivative of pK19mobsacB for <i>ureD</i> gene truncation by replacing Glu188 in <i>ureD</i> with the stop codon	R. Mahr et al. (33)
pJC1	Kan ^r <i>oriV_{Ec}</i> <i>oriV_{Cg}</i> ; <i>E. coli</i> - <i>C. glutamicum</i> shuttle vector	J. Cremer et al. (79)
pJC1- <i>venus</i> -term-BS	Kan ^r ; derivative of pJC1, containing the terminator sequence of <i>Bacillus subtilis</i> behind <i>venus</i>	M. Baumgart et al. (74)
pJC1- <i>pyc</i>	Kan ^r ; derivative of pJC1- <i>venus</i> -term-BS, containing <i>pyc</i> under the control of its native promoter <i>P_{pyc}</i>	This work
pJC1- <i>P_{tac}</i> - <i>aceA</i> - <i>aceB</i>	Kan ^r ; derivative of pJC1- <i>venus</i> -term-BS, containing <i>lacI</i> and <i>aceA</i> followed by a linking sequence (5'-ACTAGAAATAATTTTGTAACTTTAAGAAGGAGATATACAT-3') and <i>aceB</i> under the control of the inducible promoter <i>P_{tac}</i>	This work
pJC1- <i>P_{tac}</i> - <i>aceB</i> - <i>aceA</i>	Kan ^r ; derivative of pJC1- <i>venus</i> -term-BS, containing <i>lacI</i> and <i>aceB</i> followed by a linking sequence (5'-ACTAGAAATAATTTTGTAACTTTAAGAAGGAGATATACAT-3') and <i>aceA</i> under the control of the inducible promoter <i>P_{tac}</i>	This work

Microtiter plate cultivation. Online monitoring of growth and/or pH was performed in 48-well microtiter FlowerPlates (m2p-labs GmbH, Baesweiler, Germany) sealed with sterile breathable rayon film (VWR International, PA) in a BioLector microtiter cultivation system (m2p-labs GmbH, Baesweiler, Germany) (65). The cultivation conditions were adjusted as described previously (66), and biomass formation was recorded every 15 min as the backscattered light intensity (light wavelength, 620 nm; signal gain factor of 20) for 24 to 72 h at 30°C and 1,200 rpm. pH measurements were performed with 48-well microtiter FlowerPlates equipped with pH optodes. The data obtained were evaluated using BioLector (m2p-labs, Baesweiler, Germany) and GraphPad Prism 7 (GraphPad Software, Inc., San Diego, CA) software.

ALE. Adaptive laboratory evolution (ALE) of *C. glutamicum* $\Delta aceE$ and *C. glutamicum* $\Delta aceE \Delta pyc$ was performed in deep-well plates (VWR International, PA) in a main culture of 1 ml CGXII medium containing either 154 mM acetate and 222 mM glucose or solely 154 mM acetate (as a control without selection pressure) adjusted to an OD₆₀₀ of 1. Cells were cultivated for 2 to 3 days before the next generation was inoculated, starting at an OD₆₀₀ of 1, and cultivated again for 2 to 3 days. After each generation step, glycerol stocks of cultures were prepared (20% glycerol) and were stored at −80°C, allowing growth analysis and DNA sequencing of cultures from individual inoculations. In total, 16 serial transfers were analyzed.

Cloning techniques and recombinant DNA work. Standard molecular biology methods were performed according to J. Sambrook and D. W. Russell (67). *C. glutamicum* ATCC 13032 chromosomal DNA was used as the template for PCR amplification of DNA fragments and was prepared as described previously (68). DNA fragment and plasmid sequencing, as well as synthesis of oligonucleotides, was performed by Eurofins Genomics (Ebersberg, Germany).

For the construction of plasmids (see Table S3 in the supplemental material), DNA fragments were amplified using the respective oligonucleotides (see Table S4) and were enzymatically assembled into a vector backbone according to reference 69.

To achieve genomic deletion of *pyc*, *ptsG*, *ppc*, and *pgi*, two-step homologous recombination using the pK19mobsacB system (70) was implemented. The suicide plasmids (compare Table 7 with Table S2 in the supplemental material) were isolated from *E. coli* cells using the QIAprep spin miniprep kit (Qiagen, Hilden, Germany). Electrocompetent *C. glutamicum* $\Delta aceE$ and *C. glutamicum* $\Delta aceE \Delta pyc$ cells were transformed with these plasmids by electroporation (71). The first and second recombination events were performed and verified as described in previous studies (72). The deletion of *pyc*, *ptsG*, *ppc*, and *pgi* was reviewed by amplification and sequencing using primers shown in Table S1.

Measurement of glucose concentrations. To measure the glucose concentration of the culture medium at different time points, cultivation was performed in 50 ml in shaking flasks. During cultivation, 0.5-ml samples were taken every 3 h and were centrifuged (16,000 × *g*). The supernatant was collected and was stored at −20°C until use.

The actual glucose concentration was measured using a D-glucose UV test kit (R-Biopharm, Darmstadt, Germany), and calculations were done, according to the manufacturer's instructions. Absorption was measured at 340 nm.

Further calculations of the glucose uptake rates could be done based on the glucose concentrations and OD₆₀₀ values obtained. According to reference 18, the following equation was used to determine the glucose concentration in nanomoles per gram (dry weight) per hour:

$$\left(\frac{S}{M} \right) \cdot \mu \cdot \left[\left(\frac{\text{nmol} \cdot \text{liter}^{-1} \cdot \text{OD}_{600}^{-1}}{\text{gDW} \cdot \text{liter}^{-1} \cdot \text{OD}_{600}^{-1}} \right) \cdot \text{h}^{-1} \right] = \left[\frac{\text{nmol}}{\text{gDW} \cdot \text{h}} \right]$$

where *S* represents the slope of the glucose concentration versus the OD₆₀₀ (expressed as nanomoles per liter per OD₆₀₀ unit), *M* is the correlation between the dry weight and the OD₆₀₀ (expressed in grams [dry weight] per liter per OD₆₀₀ unit), and μ is the growth rate per hour. According to A. Kabus et al. (73), an OD₆₀₀ of 1 corresponds to 0.25 g (dry weight) liter^{−1}, so this value was used as *M* throughout these calculations.

Quantification of amino acid production. Using ultrahigh-performance liquid chromatography (uHPLC), amino acids were quantified as *ortho*-phthalaldehyde derivatives by automatic precolumn derivatization. Derivatives were separated by reverse-phase chromatography on an Agilent (Santa Clara, CA) 1290 Infinity LC ChemStation equipped with a fluorescence detector. As the eluent for the Zorbax Eclipse amino acid analysis (AAA) column (particle size, 3.5 μ m; inside diameter, 4.6 mm; length, 75 mm; Agilent, Santa Clara, CA), a gradient of Na-borate buffer (10 mM Na₂HPO₄, 10 mM Na₂B₄O₇ [pH 8.2]; adapted to operator's guide) and methanol was applied. Prior to analysis, samples were centrifuged for 10 min at 16,000 × *g* and 4°C and were diluted 1:100.

Monitoring of cellular proliferation by cell staining. For the staining of proliferating cells, the PKH67 green fluorescent cell linker kit for general cell membrane labeling (Sigma-Aldrich, Munich, Germany) was used, and the protocol was adapted according to the work of O. Kotte et al. (35). From an exponentially growing preculture in CGXII minimal medium containing 222 mM glucose and 154 mM acetate, 1.5 × 10⁹ cells were harvested by centrifugation for 4 min at 4,000 × *g* and 4°C. Then the cells were washed again in 5 ml ice-cold CGXII basic solution, without MgSO₄, CaCl₂, biotin, trace elements, or protocatechuic acid. For staining, the cell pellet was resuspended in 500 μ l dilution buffer C (Sigma-Aldrich, Munich, Germany) at room temperature, and a freshly prepared mixture of 10 μ l PKH67 dye (Sigma-Aldrich, Munich, Germany) and 500 μ l dilution buffer C was added. Subsequently, cells were incubated for 3 min at room temperature, and afterwards, 4 ml ice-cold filtered CGXII basic solution containing 1% (wt/vol) bovine serum albumin, 1 mM MgSO₄, and 0.1 mM CaCl₂ was added. Then the cells were centrifuged for 4 min at 4,000 × *g* and 4°C, and the cell pellet was washed twice. Finally, the cells

were resuspended in CGXII minimal medium containing 222 mM glucose and 154 mM acetate and were cultivated in a microtiter cultivation system.

Flow cytometry. Flow cytometric (FC) analyses were conducted on a FACSaria II flow cytometer (Becton, Dickinson, San Jose, CA) equipped with a blue solid-state laser (excitation, 488 nm). Forward-scatter characteristics (FSC) and side-scatter characteristics (SSC) were recorded as small-angle and orthogonal scatters of the 488-nm laser, respectively. PKH67 fluorescence was detected using a 502-nm long-pass and 530/30-nm band-pass filter set. FACSDiva software, version 6.0, was used to monitor the measurements. During analyses, thresholding on FSC was applied to remove background noise. For FC analyses, PKH67-stained culture samples were diluted to an OD₆₀₀ of 0.05 in FACSFlow sheath fluid buffer (BD, Heidelberg, Germany). FlowJo (version 10.0.8) analysis software was used to visualize and evaluate the data (Tree Star, Ashland, OR).

DNA microarrays. For analysis of the transcriptome, *C. glutamicum* $\Delta aceE$ and *C. glutamicum* $\Delta aceE \Delta pyc$ were cultivated in triplicate as described above in 50 ml CGXII medium containing 154 mM acetate and 222 mM glucose in shake flasks. After reaching exponential phase at an OD₆₀₀ of ca. 12 to 15, the cell suspension was harvested by centrifugation ($4,256 \times g$, 10 min, 4°C). The resulting pellet was directly frozen in liquid nitrogen and was stored at -80°C . RNA preparation and cDNA synthesis, as well as microchip hybridization, scanning, and evaluation, were performed as described in previous studies (74).

GC-ToF MS analysis. For analysis of the metabolome, samples of *C. glutamicum* $\Delta aceE$ in the exponential phase, as well as samples of *C. glutamicum* $\Delta aceE \Delta pyc$ in the stationary and exponential phases, were taken, and cells were disrupted using hot methanol. Further sample preparation, derivatization, mass spectrometry (MS) operation, and peak identification were accomplished according to the method of N. Paczia et al. (75) in an Agilent (Santa Clara, CA) 6890N gas chromatograph coupled to a Waters (Milford, MA) Micromass GCT Premier high-resolution ToF MS. Known metabolites were identified using the in-house database JuPoD, the commercial database NIST17 (National Institute of Standards and Technology, USA), and the GMD database (Max Planck Institute of Molecular Plant Physiology, Golm, Germany) (76).

Whole-genome sequencing. In order to sequence the whole genome of *C. glutamicum* $\Delta aceE \Delta pyc$ mutants from the ALE experiment using next-generation sequencing (NGS), genomic DNA was prepared using the NucleoSpin microbial DNA kit (Macherey-Nagel, Düren, Germany) according to the manufacturer's instructions. Subsequently, the concentrations of the purified genomic DNA were measured using a Qubit 2.0 fluorometer (Invitrogen, Carlsbad, CA) according to the manufacturer's instructions. Overall, 4 μg purified genomic DNA was employed for the preparation for genome sequencing using a TruSeq DNA library prep kit and a MiSeq reagent kit, version 1 (Illumina, San Diego, CA, USA), according to the manufacturer's instructions. The sequencing run was performed in a MiSeq system (Illumina, San Diego, CA). Data analysis and base calling were performed with the Illumina instrument software. The resulting FASTQ output files were examined using CLC Genomics Workbench 9 (Qiagen, Aarhus, Denmark).

Accession number(s). The microarray data determined in this study are available at NCBI's Gene Expression Omnibus under accession number [GSE134218](https://www.ncbi.nlm.nih.gov/geo/query/acc.cgi?acc=GSE134218).

SUPPLEMENTAL MATERIAL

Supplemental material for this article may be found at <https://doi.org/10.1128/JB.00387-19>.

SUPPLEMENTAL FILE 1, PDF file, 1.4 MB.

ACKNOWLEDGMENTS

We thank Jochem Gätgens for performing GC-ToF analyses, and we thank Bastian Blombach and Stephan Noack for fruitful discussions.

We acknowledge financial support by the Helmholtz Association (grant W2/W3-096).

REFERENCES

- Bailey JE, Ollis DF. 1986. Biochemical engineering fundamentals. McGraw-Hill, New York, NY.
- Blombach B, Takors R. 2015. CO₂—intrinsic product, essential substrate, and regulatory trigger of microbial and mammalian production processes. Front Bioeng Biotechnol 3:108. <https://doi.org/10.3389/fbioe.2015.00108>.
- de Kok A, Hengeveld AF, Martin A, Westphal AH. 1998. The pyruvate dehydrogenase multi-enzyme complex from Gram-negative bacteria. Biochim Biophys 1385:353–366. [https://doi.org/10.1016/S0167-4838\(98\)00079-X](https://doi.org/10.1016/S0167-4838(98)00079-X).
- Eikmanns BJ, Blombach B. 2014. The pyruvate dehydrogenase complex of *Corynebacterium glutamicum*: an attractive target for metabolic engineering. J Biotechnol 192(Pt B):339–345. <https://doi.org/10.1016/j.jbiotec.2013.12.019>.
- Schreiner ME, Fiur D, Holátko J, Pátek M, Eikmanns BJ. 2005. E1 enzyme of the pyruvate dehydrogenase complex in *Corynebacterium glutamicum*: molecular analysis of the gene and phylogenetic aspects. J Bacteriol 187:6005–6018. <https://doi.org/10.1128/JB.187.17.6005-6018.2005>.
- Becker J, Rohles CM, Wittmann C. 2018. Metabolically engineered *Corynebacterium glutamicum* for bio-based production of chemicals, fuels, materials, and healthcare products. Metab Eng 50:122–141. <https://doi.org/10.1016/j.jymben.2018.07.008>.
- Kogure T, Inui M. 2018. Recent advances in metabolic engineering of *Corynebacterium glutamicum* for bioproduction of value-added aromatic chemicals and natural products. Appl Microbiol Biotechnol 102:8685–8705. <https://doi.org/10.1007/s00253-018-9289-6>.
- Wang X, Zhang H, Quinn PJ. 2018. Production of L-valine from metabolically engineered *Corynebacterium glutamicum*. Appl Microbiol Biotechnol 102:4319–4330. <https://doi.org/10.1007/s00253-018-8952-2>.
- Wendisch VF, Mindt M, Pérez-García F. 2018. Biotechnological production of mono- and diamines using bacteria: recent progress, applications, and perspectives. Appl Microbiol Biotechnol 102:3583–3594. <https://doi.org/10.1007/s00253-018-8890-z>.

10. Eggeling L, Bott M. 2005. Handbook of *Corynebacterium glutamicum*. Academic Press, Boca Raton, FL.
11. Blombach B, Schreiner ME, Bartek T, Oldiges M, Eikmanns BJ. 2008. *Corynebacterium glutamicum* tailored for high-yield L-valine production. Appl Microbiol Biotechnol 79:471–479. <https://doi.org/10.1007/s00253-008-1444-z>.
12. Blombach B, Schreiner ME, Holatko J, Bartek T, Oldiges M, Eikmanns BJ. 2007. L-Valine production with pyruvate dehydrogenase complex-deficient *Corynebacterium glutamicum*. Appl Environ Microbiol 73: 2079–2084. <https://doi.org/10.1128/AEM.02826-06>.
13. Buchholz J, Schwentner A, Brunnenkan B, Gabris C, Grimm S, Gerstmeir R, Takors R, Eikmanns BJ, Blombach B. 2013. Platform engineering of *Corynebacterium glutamicum* with reduced pyruvate dehydrogenase complex activity for improved production of L-lysine, L-valine, and 2-ketoisovalerate. Appl Environ Microbiol 79:5566–5575. <https://doi.org/10.1128/AEM.01741-13>.
14. Coccagn M, Monnet C, Lindley ND. 1993. Batch kinetics of *Corynebacterium glutamicum* during growth on various carbon substrates: use of substrate mixtures to localise metabolic bottlenecks. Appl Microbiol Biotechnol 40:526–530. <https://doi.org/10.1007/BF00175743>.
15. Wendisch VF, de Graaf AA, Sahm H, Eikmanns BJ. 2000. Quantitative determination of metabolic fluxes during cointilization of two carbon sources: comparative analyses with *Corynebacterium glutamicum* during growth on acetate and/or glucose. J Bacteriol 182:3088–3096. <https://doi.org/10.1128/JB.182.11.3088-3096.2000>.
16. Dominguez H, Coccagn-Bousquet M, Lindley ND. 1997. Simultaneous consumption of glucose and fructose from sugar mixtures during batch growth of *Corynebacterium glutamicum*. Appl Microbiol Biotechnol 47: 600–603. <https://doi.org/10.1007/s002530050980>.
17. Stansen C, Uy D, Delaunay S, Eggeling L, Goergen J-L, Wendisch VF. 2005. Characterization of a *Corynebacterium glutamicum* lactate utilization operon induced during temperature-triggered glutamate production. Appl Environ Microbiol 71:5920–5928. <https://doi.org/10.1128/AEM.71.10.5920-5928.2005>.
18. Frunzke J, Engels V, Hasenbein S, Gätgens C, Bott M. 2008. Co-ordinated regulation of gluconate catabolism and glucose uptake in *Corynebacterium glutamicum* by two functionally equivalent transcriptional regulators, GntR1 and GntR2. Mol Microbiol 67:305–322. <https://doi.org/10.1111/j.1365-2958.2007.06020.x>.
19. Wendisch VF, Spies M, Reinscheid DJ, Schnicke S, Sahm H, Eikmanns BJ. 1997. Regulation of acetate metabolism in *Corynebacterium glutamicum*: transcriptional control of the isocitrate lyase and malate synthase genes. Arch Microbiol 168:262–269. <https://doi.org/10.1007/s002030050497>.
20. Sauer U, Eikmanns BJ. 2005. The PEP-pyruvate-oxaloacetate node as the switch point for carbon flux distribution in bacteria. FEMS Microbiol Rev 29:765–794. <https://doi.org/10.1016/j.femsre.2004.11.002>.
21. Eikmanns BJ, Follettie MT, Griot MU, Sinskey AJ. 1989. The phosphoenolpyruvate carboxylase gene of *Corynebacterium glutamicum*: molecular cloning, nucleotide sequence, and expression. Mol Gen Genet 218: 330–339. <https://doi.org/10.1007/BF00331286>.
22. O'Regan M, Thierbach G, Bachmann B, Villevall D, Lepage P, Viret JF, Lemoine Y. 1989. Cloning and nucleotide sequence of the phosphoenolpyruvate carboxylase-coding gene of *Corynebacterium glutamicum* ATCC13032. Gene 77:237–251. [https://doi.org/10.1016/0378-1119\(89\)90072-3](https://doi.org/10.1016/0378-1119(89)90072-3).
23. Peters-Wendisch PG, Kreutzer C, Kalinowski J, Patek M, Sahm H, Eikmanns BJ. 1998. Pyruvate carboxylase from *Corynebacterium glutamicum*: characterization, expression and inactivation of the *pyc* gene. Microbiology 144: 915–927. <https://doi.org/10.1099/00221287-144-4-915>.
24. Kai Y, Matsumura H, Inoue T, Terada K, Nagara Y, Yoshinaga T, Kihara A, Tsumura K, Izui K. 1999. Three-dimensional structure of phosphoenolpyruvate carboxylase: a proposed mechanism for allosteric inhibition. Proc Natl Acad Sci U S A 96:823–828. <https://doi.org/10.1073/pnas.96.3.823>.
25. Repaske R, Repaske AC, Mayer RD. 1974. Carbon dioxide control of lag period and growth of *Streptococcus sanguis*. J Bacteriol 117:652–659.
26. Talley RS, Baugh CL. 1975. Effects of bicarbonate on growth of *Neisseria gonorrhoeae*: replacement of gaseous CO₂ atmosphere. Appl Microbiol 29:469–471.
27. Bäumchen C, Knoll A, Husemann B, Seletzky J, Maier B, Dietrich C, Amoabediny G, Buchs J. 2007. Effect of elevated dissolved carbon dioxide concentrations on growth of *Corynebacterium glutamicum* on D-glucose and L-lactate. J Biotechnol 128:868–874. <https://doi.org/10.1016/j.jbiotec.2007.01.001>.
28. Blombach B, Buchholz J, Busche T, Kalinowski J, Takors R. 2013. Impact of different CO₂/HCO₃⁻ levels on metabolism and regulation in *Corynebacterium glutamicum*. J Biotechnol 168:331–340. <https://doi.org/10.1016/j.jbiotec.2013.10.005>.
29. Bartek T, Blombach B, Lang S, Eikmanns BJ, Wiechert W, Oldiges M, Noh K, Noack S. 2011. Comparative ¹³C metabolic flux analysis of pyruvate dehydrogenase complex-deficient, L-valine-producing *Corynebacterium glutamicum*. Appl Environ Microbiol 77:6644–6652. <https://doi.org/10.1128/AEM.00575-11>.
30. Dominguez H, Lindley ND. 1996. Complete sucrose metabolism requires fructose phosphotransferase activity in *Corynebacterium glutamicum* to ensure phosphorylation of liberated fructose. Appl Environ Microbiol 62:3878–3880.
31. Moon MW, Kim HJ, Oh TK, Shin CS, Lee JS, Kim SJ, Lee JK. 2005. Analyses of enzyme II gene mutants for sugar transport and heterologous expression of fructokinase gene in *Corynebacterium glutamicum* ATCC 13032. FEMS Microbiol Lett 244:259–266. <https://doi.org/10.1016/j.femsle.2005.01.053>.
32. Peters-Wendisch PG, Eikmanns BJ, Thierbach G, Bachmann B, Sahm H. 1993. Phosphoenolpyruvate carboxylase in *Corynebacterium glutamicum* is dispensable for growth and lysine production. FEMS Microbiol Lett 112:269–274. <https://doi.org/10.1111/j.1574-6968.1993.tb06461.x>.
33. Mahr R, Gätgens C, Gätgens J, Polen T, Kalinowski J, Frunzke J. 2015. Biosensor-driven adaptive laboratory evolution of L-valine production in *Corynebacterium glutamicum*. Metab Eng 32:184–194. <https://doi.org/10.1016/j.ymben.2015.09.017>.
34. Reinscheid DJ, Eikmanns BJ, Sahm H. 1994. Characterization of the isocitrate lyase gene from *Corynebacterium glutamicum* and biochemical analysis of the enzyme. J Bacteriol 176:3474–3483. <https://doi.org/10.1128/jb.176.12.3474-3483.1994>.
35. Kotte O, Volkmer B, Radzikowski JL, Heinemann M. 2014. Phenotypic bistability in *Escherichia coli*'s central carbon metabolism. Mol Syst Biol 10:736. <https://doi.org/10.15252/msb.20135022>.
36. Takhaviev V, Heinemann M. 2018. Metabolic heterogeneity in clonal microbial populations. Curr Opin Microbiol 45:30–38. <https://doi.org/10.1016/j.mib.2018.02.004>.
37. Heinemann M, Zenobi R. 2011. Single cell metabolomics. Curr Opin Biotechnol 22:26–31. <https://doi.org/10.1016/j.copbio.2010.09.008>.
38. Davis KM, Isberg RR. 2016. Defining heterogeneity within bacterial populations via single cell approaches. Bioessays 38:782–790. <https://doi.org/10.1002/bies.201500121>.
39. Ikeda M, Mizuno Y, Awane SI, Hayashi M, Mitsuhashi S, Takeno S. 2011. Identification and application of a different glucose uptake system that functions as an alternative to the phosphotransferase system in *Corynebacterium glutamicum*. Appl Microbiol Biotechnol 90:1443–1451. <https://doi.org/10.1007/s00253-011-3210-x>.
40. Lindner SN, Seibold GM, Henrich A, Krämer R, Wendisch VF. 2011. Phosphotransferase system-independent glucose utilization in *Corynebacterium glutamicum* by inositol permeases and glucokinases. Appl Environ Microbiol 77:3571–3581. <https://doi.org/10.1128/AEM.02713-10>.
41. Peters-Wendisch PG, Schiel B, Wendisch VF, Katsoulidis E, Mockel B, Sahm H, Eikmanns BJ. 2001. Pyruvate carboxylase is a major bottleneck for glutamate and lysine production by *Corynebacterium glutamicum*. J Mol Microbiol Biotechnol 3:295–300.
42. Kortmann M, Mack C, Baumgart M, Bott M. 2019. Pyruvate carboxylase variants enabling improved lysine production from glucose identified by biosensor-based high-throughput fluorescence-activated cell sorting screening. ACS Synth Biol 8:274–281. <https://doi.org/10.1021/acssynbio.8b00510>.
43. Chatterjee R, Millard CS, Champion K, Clark DP, Donnelly MI. 2001. Mutation of the *ptsG* gene results in increased production of succinate in fermentation of glucose by *Escherichia coli*. Appl Environ Microbiol 67:148–154. <https://doi.org/10.1128/AEM.67.1.148-154.2001>.
44. Wang Q, Wu C, Chen T, Chen X, Zhao X. 2006. Expression of galactose permease and pyruvate carboxylase in *Escherichia coli ptsG* mutant increases the growth rate and succinate yield under anaerobic conditions. Biotechnol Lett 28:89–93. <https://doi.org/10.1007/s10529-005-4952-2>.
45. Vanderpool CK, Gottesman S. 2007. The novel transcription factor SgrR coordinates the response to glucose-phosphate stress. J Bacteriol 189: 2238–2248. <https://doi.org/10.1128/JB.01689-06>.
46. Morita T, El-Kazzaz W, Tanaka Y, Inada T, Aiba H. 2003. Accumulation of glucose 6-phosphate or fructose 6-phosphate is responsible for destabilization of glucose transporter mRNA in *Escherichia coli*. J Biol Chem 278:15608–15614. <https://doi.org/10.1074/jbc.M300177200>.

47. Kadner RJ, Murphy GP, Stephens CM. 1992. Two mechanisms for growth inhibition by elevated transport of sugar phosphates in *Escherichia coli*. *J Gen Microbiol* 138:2007–2014. <https://doi.org/10.1099/00221287-138-10-2007>.
48. Kessler JR, Cobe BL, Richards GR. 2017. Stringent response regulators contribute to recovery from glucose phosphate stress in *Escherichia coli*. *Appl Environ Microbiol* 83:e01636–17. <https://doi.org/10.1128/aem.01636-17>.
49. Vanderpool CK, Gottesman S. 2004. Involvement of a novel transcriptional activator and small RNA in post-transcriptional regulation of the glucose phosphoenolpyruvate phosphotransferase system. *Mol Microbiol* 54:1076–1089. <https://doi.org/10.1111/j.1365-2958.2004.04348.x>.
50. Engels V, Wendisch VF. 2007. The DeoR-type regulator SugR represses expression of *ptsG* in *Corynebacterium glutamicum*. *J Bacteriol* 189:2955–2966. <https://doi.org/10.1128/JB.01596-06>.
51. Gaigalat L, Schlüter JP, Hartmann M, Mormann S, Tauch A, Pühler A, Kalinowski J. 2007. The DeoR-type transcriptional regulator SugR acts as a repressor for genes encoding the phosphoenolpyruvate:sugar phosphotransferase system (PTS) in *Corynebacterium glutamicum*. *BMC Mol Biol* 8:104. <https://doi.org/10.1186/1471-2199-8-104>.
52. Tanaka Y, Teramoto H, Inui M, Yukawa H. 2008. Regulation of expression of general components of the phosphoenolpyruvate:carbohydrate phosphotransferase system (PTS) by the global regulator SugR in *Corynebacterium glutamicum*. *Appl Microbiol Biotechnol* 78:309–318. <https://doi.org/10.1007/s00253-007-1313-1>.
53. Blombach B, Arndt A, Auchter M, Eikmanns BJ. 2009. L-Valine production during growth of pyruvate dehydrogenase complex-deficient *Corynebacterium glutamicum* in the presence of ethanol or by inactivation of the transcriptional regulator SugR. *Appl Environ Microbiol* 75:1197–1200. <https://doi.org/10.1128/AEM.02351-08>.
54. Repaske R, Clayton MA. 1978. Control of *Escherichia coli* growth by CO₂. *J Bacteriol* 135:1162–1164.
55. Valley G, Rettger LF. 1927. The influence of carbon dioxide on bacteria. *J Bacteriol* 14:101–137.
56. Bracher JM, Martinez-Rodriguez OA, Dekker WJC, Verhoeven MD, van Maris AJA, Pronk JT. 2019. Reassessment of requirements for anaerobic xylose fermentation by engineered, non-evolved *Saccharomyces cerevisiae* strains. *FEMS Yeast Res* 19. <https://doi.org/10.1093/femsyr/foy104>.
57. Gonzalez JE, Long CP, Antoniewicz MR. 2017. Comprehensive analysis of glucose and xylose metabolism in *Escherichia coli* under aerobic and anaerobic conditions by ¹³C metabolic flux analysis. *Metab Eng* 39:9–18. <https://doi.org/10.1016/j.ymben.2016.11.003>.
58. Gerstmeier R, Cramer A, Dangel P, Schaffer S, Eikmanns BJ. 2004. RamB, a novel transcriptional regulator of genes involved in acetate metabolism of *Corynebacterium glutamicum*. *J Bacteriol* 186:2798–2809. <https://doi.org/10.1128/JB.186.9.2798-2809.2004>.
59. Cramer A, Gerstmeier R, Schaffer S, Bott M, Eikmanns BJ. 2006. Identification of RamA, a novel LuxR-type transcriptional regulator of genes involved in acetate metabolism of *Corynebacterium glutamicum*. *J Bacteriol* 188:2554–2567. <https://doi.org/10.1128/JB.188.7.2554-2567.2006>.
60. Kornberg HL. 1966. The role and control of the glyoxylate cycle in *Escherichia coli*. *Biochem J* 99:1–11. <https://doi.org/10.1042/bj0990001>.
61. MacKintosh C, Nimmo HG. 1988. Purification and regulatory properties of isocitrate lyase from *Escherichia coli* ML308. *Biochem J* 250:25–31. <https://doi.org/10.1042/bj2500025>.
62. Robertson EF, Reeves HC. 1986. Purification and characterization of isocitrate lyase from *Escherichia coli*. *Curr Microbiol* 14:347–350. <https://doi.org/10.1007/BF01568702>.
63. Kalinowski J, Bathe B, Bartels D, Bischoff N, Bott M, Burkovski A, Dusch N, Eggeling L, Eikmanns BJ, Gaigalat L, Goesmann A, Hartmann M, Huthmacher K, Krämer R, Linke B, McHardy AC, Meyer F, Möckel B, Pfeifferle W, Pühler A, Rey DA, Rückert C, Rupp O, Sahl H, Wendisch VF, Wiegräbe I, Tauch A. 2003. The complete *Corynebacterium glutamicum* ATCC 13032 genome sequence and its impact on the production of L-aspartate-derived amino acids and vitamins. *J Biotechnol* 104:5–25. [https://doi.org/10.1016/S0168-1656\(03\)00154-8](https://doi.org/10.1016/S0168-1656(03)00154-8).
64. Keilhauer C, Eggeling L, Sahl H. 1993. Isoleucine synthesis in *Corynebacterium glutamicum*: molecular analysis of the *ilvB-ilvN-ilvC* operon. *J Bacteriol* 175:5595–5603. <https://doi.org/10.1128/jb.175.17.5595-5603.1993>.
65. Kensey F, Zang E, Faulhammer C, Tan RK, Büchs J. 2009. Validation of a high-throughput fermentation system based on online monitoring of biomass and fluorescence in continuously shaken microtiter plates. *Microb Cell Fact* 8:31. <https://doi.org/10.1186/1475-2859-8-31>.
66. Mustafi N, Grünberger A, Kohlheyer D, Bott M, Frunzke J. 2012. The development and application of a single-cell biosensor for the detection of L-methionine and branched-chain amino acids. *Metab Eng* 14:449–457. <https://doi.org/10.1016/j.ymben.2012.02.002>.
67. Sambrook J, Russell DW. 2001. Molecular cloning: a laboratory manual, 3rd ed. Cold Spring Harbor Laboratory Press, Cold Spring Harbor, NY.
68. Eikmanns BJ, Thum-Schmitz N, Eggeling L, Ludtke K-U, Sahl H. 1994. Nucleotide sequence, expression and transcriptional analysis of the *Corynebacterium glutamicum* *gltA* gene encoding citrate synthase. *Microbiology* 140:1817–1828. <https://doi.org/10.1099/13500872-140-8-1817>.
69. Gibson DG, Young L, Chuang RY, Venter JC, Hutchison CA, Smith HO. 2009. Enzymatic assembly of DNA molecules up to several hundred kilobases. *Nat Methods* 6:343–345. <https://doi.org/10.1038/nmeth.1318>.
70. Schäfer A, Tauch A, Jäger W, Kalinowski J, Thierbach G, Pühler A. 1994. Small mobilizable multi-purpose cloning vectors derived from the *Escherichia coli* plasmids pK18 and pK19: selection of defined deletions in the chromosome of *Corynebacterium glutamicum*. *Gene* 145:69–73. [https://doi.org/10.1016/0378-1119\(94\)90324-7](https://doi.org/10.1016/0378-1119(94)90324-7).
71. van der Rest ME, Lange C, Molenaar D. 1999. A heat shock following electroporation induces highly efficient transformation of *Corynebacterium glutamicum* with xenogeneic plasmid DNA. *Appl Microbiol Biotechnol* 52:541–545. <https://doi.org/10.1007/s002530051557>.
72. Niebisch A, Bott M. 2001. Molecular analysis of the cytochrome *bc₁-aa₃* branch of the *Corynebacterium glutamicum* respiratory chain containing an unusual diheme cytochrome *c₁*. *Arch Microbiol* 175:282–294. <https://doi.org/10.1007/s002030100262>.
73. Kabus A, Georgi T, Wendisch VF, Bott M. 2007. Expression of the *Escherichia coli* *pntAB* genes encoding a membrane-bound transhydrogenase in *Corynebacterium glutamicum* improves L-lysine formation. *Appl Microbiol Biotechnol* 75:47–53. <https://doi.org/10.1007/s00253-006-0804-9>.
74. Baumgart M, Luder K, Grover S, Gätgens C, Besra GS, Frunzke J. 2013. IpsA, a novel LacI-type regulator, is required for inositol-derived lipid formation in *Corynebacteria* and *Mycobacteria*. *BMC Biol* 11:122. <https://doi.org/10.1186/1741-7007-11-122>.
75. Paczia N, Nilgen A, Lehmann T, Gätgens J, Wiechert W, Noack S. 2012. Extensive exometabolome analysis reveals extended overflow metabolism in various microorganisms. *Microb Cell Fact* 11:122. <https://doi.org/10.1186/1475-2859-11-122>.
76. Hummel J, Strehmel N, Selbig J, Walther D, Kopka J. 2010. Decision tree supported substructure prediction of metabolites from GC-MS profiles. *Metabolomics* 6:322–333. <https://doi.org/10.1007/s11306-010-0198-7>.
77. Kinoshita S, Udaka S, Shimono M. 2004. Studies on the amino acid fermentation. Part 1. Production of L-glutamic acid by various microorganisms. *J Gen Appl Microbiol* 50:331–343.
78. Schwentner A, Feith A, Münch E, Busche T, Rückert C, Kalinowski J, Takors R, Blombach B. 2018. Metabolic engineering to guide evolution: creating a novel mode for L-valine production with *Corynebacterium glutamicum*. *Metab Eng* 47:31–41. <https://doi.org/10.1016/j.ymben.2018.02.015>.
79. Cremer J, Eggeling L, Sahl H. 1990. Cloning the *dapA* *dapB* cluster of the lysine-secreting bacterium *Corynebacterium glutamicum*. *Mol Gen Genet* 220:478–480. <https://doi.org/10.1007/BF00391757>.